RESEARCH PAPER

BJP | BRITISH PHARMACOLOGICAL SOCIETY

Activation of pregnane X receptor induces atherogenic lipids and PCSK9 by a SREBP2-mediated mechanism

Mikko Karpale[1,2,3] | Aki Juhani Käräjämäki[2,4,5] | Outi Kummu[1,2,3] |
Helena Gylling[6] | Tuulia Hyötyläinen[7] | Matej Orešič[8,9] | Ari Tolonen[10] |
Heidi Hautajärvi[10] | Markku J. Savolainen[2,3,13] | Mika Ala-Korpela[3,11,12] |
Janne Hukkanen[2,3,13] | Jukka Hakkola[1,2,3]

[1]Research Unit of Biomedicine, University of Oulu, Oulu, Finland

[2]Medical Research Center, Oulu University Hospital and University of Oulu, Oulu, Finland

[3]Biocenter Oulu, University of Oulu, Oulu, Finland

[4]Department of gastroenterology, Clinics of Internal Medicine, Vaasa Central Hospital, Vaasa, Finland

[5]Abdominal Center, Department of Internal Medicine, Oulu University Hospital, Oulu, Finland

[6]Heart and Lung Center, University of Helsinki and Helsinki University Central Hospital, Helsinki, Finland

[7]School of Science and Technology, Örebro University, Örebro, Sweden

[8]School of Medical Sciences, Örebro University, Örebro, Sweden

[9]Turku Bioscience Centre, University of Turku and Åbo Akademi University, Turku, Finland

[10]Admescope Ltd., Oulu, Finland

[11]Computational Medicine, Faculty of Medicine, University of Oulu and Biocenter Oulu, Oulu, Finland

[12]NMR Metabolomics Laboratory, School of Pharmacy, University of Eastern Finland, Kuopio, Finland

[13]Research Unit of Internal Medicine, University of Oulu, Oulu, Finland

Correspondence
Janne Hukkanen, Research Unit of Internal Medicine, and Jukka Hakkola, Research Unit of Biomedicine, University of Oulu, Oulu, Finland.
Email: janne.hukkanen@oulu.fi; jukka.hakkola@oulu.fi

Background and Purpose: Many drugs and environmental contaminants induce hypercholesterolemia and promote the risk of atherosclerotic cardiovascular disease. We tested the hypothesis that pregnane X receptor (PXR), a xenobiotic-sensing nuclear receptor, regulates the level of circulating atherogenic lipids in humans and utilized mouse experiments to identify the mechanisms involved.

Experimental Approach: We performed serum NMR metabolomics in healthy volunteers administered rifampicin, a prototypical human PXR ligand or placebo in a cross-over setting. We used high-fat diet fed wild-type and PXR knockout mice to investigate the mechanisms mediating the PXR-induced alterations in cholesterol homeostasis.

Key Results: Activation of PXR induced cholesterogenesis both in pre-clinical and clinical settings. In human volunteers, rifampicin increased intermediate-density lipoprotein (IDL), low-density lipoprotein (LDL) and total cholesterol and lathosterol–cholesterol ratio, a marker of cholesterol synthesis, suggesting increased cholesterol synthesis. Experiments in mice indicated that PXR activation causes widespread induction of the cholesterol synthesis genes including the rate-limiting *Hmgcr* and upregulates the intermediates in the Kandutsch–Russell cholesterol synthesis pathway in the liver. Additionally, PXR activation induced plasma proprotein convertase subtilisin/kexin type 9 (PCSK9), a negative regulator of hepatic LDL uptake, in both mice and humans. We propose that these effects were mediated through increased proteolytic activation of sterol regulatory element-binding protein 2 (SREBP2) in response to PXR activation.

Conclusion and Implications: PXR activation induces cholesterol synthesis, elevating LDL and total cholesterol in humans. The PXR–SREBP2 pathway is a novel regulator of the cholesterol and PCSK9 synthesis and a molecular mechanism for drug- and chemical-induced hypercholesterolemia.

KEYWORDS

cholesterol, hypercholesterolemia, lathosterol, LDL, PCSK9, PXR, SREBP2

1 | INTRODUCTION

Hypercholesterolemia, especially high level of low-density lipoprotein (LDL) cholesterol, is one of the major risk factors for atherosclerotic cardiovascular disease, the leading global cause of mortality (G. A. Roth et al., 2015). Both inherited and acquired factors may cause hypercholesterolemia (Garg & Simha, 2007). The most common secondary causes are thought to be obesity, unhealthy diet and sedentary lifestyle (Garg & Simha, 2007). In addition, foreign compounds may affect cholesterol status.

Many drugs, including immunosuppressants, several HIV-1 antiretroviral drugs, diuretics, antiepileptics, some anabolic steroids and several antipsychotics, are known to induce hypercholesterolemia (Eirís et al., 2000; Garg & Simha, 2007; Mantel-Teeuwisse et al., 2001; Meyer & Koro, 2004). Studies in experimental animals indicate that exposure to environmental contaminants such as polychlorinated biphenyls and bisphenol A causes hypercholesterolemia (Marmugi et al., 2014; Nagaoka et al., 1990). However, the underlying mechanisms mediating the harmful cholesterol elevating effects of chemical exposure remain mostly unexplored.

Pregnane X receptor (PXR, systematic name NR1I2), is a nuclear receptor activated by a large variety of structurally divergent exogenous ligands including drugs, natural extracts and environmental chemicals (Kliewer et al., 2002). Thus, PXR is considered to play a key role in the sensing of chemical environment. Originally, PXR was found to facilitate detoxification and excretion of foreign compounds (Kliewer et al., 1998). More recently, PXR has been shown to regulate lipid metabolism (Hakkola et al., 2016; Zhou, 2016). PXR activation induces hepatic lipogenic genes and leads to liver steatosis in several

What is already known

- Exposure to different PXR ligands, such as several drugs and environmental contaminants, associates with hypercholesterolemia.
- Studies in experimental animals suggest that PXR activation induces hypercholesterolemia and accelerates atherosclerosis.

What this study adds

- Activation of PXR elevates LDL and total cholesterol in humans.
- PXR ligands increase hepatic cholesterol synthesis, plasma PCSK9 level and promote proteolytic activation of SREBP2.

What is the clinical significance

- PXR-activating drugs and environmental contaminants may pose a cardiovascular risk by increasing circulating atherogenic lipids.

animal models and lipid accumulation in human liver cell models (Bitter et al., 2015; Gwag et al., 2019; Zhou et al., 2006). Moreover, some animal studies suggest that PXR activation induces

hypercholesterolemia and accelerates atherosclerosis (Gwag et al., 2019; Meng et al., 2019; Zhou et al., 2009). Due to its wide ligand acceptance, PXR could play a major role as the mediator of cholesterogenic effect of drugs and environmental chemicals.

Interference with any of the major phases of cholesterol homeostasis, that is, synthesis, absorption, reverse cholesterol transport and excretion, could result in hypercholesterolemia (van der Wulp et al., 2013). Furthermore, the discovery of proprotein convertase subtilisin/kexin type 9 (PCSK9) has considerably changed the view of the regulation of cholesterol homeostasis. PCSK9 is a central regulator of plasma cholesterol level by influencing the levels of plasma membrane LDL receptors in hepatocytes (Warden et al., 2019). The mechanisms of PXR action remain controversial and both increased intestinal absorption and increased hepatic synthesis through activation of squalene epoxidase have recently been suggested to mediate PXR-induced hypercholesterolemia in mice (Gwag et al., 2019; Meng et al., 2019).

To address the question if PXR activation affects human cholesterol homeostasis, we analysed serum metabolomics in controlled clinical studies investigating the cardiometabolic effects of rifampicin, the prototypic human PXR ligand, and showed metabolic signature indicating increased serum cholesterol and enhanced synthesis of cholesterol. We utilized high-fat diet challenged mice as a model to reveal the mechanism mediating PXR-induced alterations in cholesterol homeostasis and showed that PXR activation induces the cholesterol synthesis pathway, increases plasma PCSK9 and promotes sterol regulatory element-binding protein 2 (SREBP2) proteolytic activation.

2 | METHODS

2.1 | Study design of the clinical trials

Three previously performed clinical trials exploring metabolic effects of rifampicin were utilized in the current study. Rifa-1 (Rysä et al., 2013) and Rifa-BP (Hassani-Nezhad-Gashti et al., 2020) studies had a randomized placebo-controlled crossover design with at least a 4-week washout period. Rifa-2 study (Hukkanen, Rysä, et al., 2015) had a one-arm design with no control arm. Rifa-1 and Rifa-2 had an open design while Rifa-BP was single-blind with study personnel blinded. The subjects (Table S1) in all three studies were administered 600-mg rifampicin (Rimapen, Orion Inc., Espoo, Finland) once a day for a week. The studies were designed to explore the effects of PXR activation on glucose tolerance (Rifa-1, $n = 12$), incretin secretion (Rifa-2, $n = 12$) and blood pressure regulation (Rifa-BP, $n = 22$). The inclusion criteria were healthy volunteers with age between 18 and 40 years (45 years in Rifa-2). The body mass index (BMI) criterion was between 19–28 kg·m^{-2} in Rifa-2 and 19–30 kg·m^{-2} in Rifa-BP, whereas Rifa-1 did not have a BMI limit. In Rifa-BP, inclusion criterion for systolic blood pressure was 95–140 mmHg, whereas the other studies did not employ blood pressure limits.

The exclusion criteria were any regular medication (hormonal intrauterine device was allowed), any major somatic or psychiatric morbidity (as judged by the study physician on the basis of history, physical examination and basic laboratory values), insensitivity to rifampicin, continuous use of soft contact lenses (rifampicin may colour), pregnancy or breast feeding, drug or alcohol abuse, history of difficult venipuncture and participation of any other medical study during the study or the past 1 month. Additionally, the diastolic blood pressure above 90 mmHg was an exclusion criterion in Rifa-BP. The original sample size calculations were targeted for fasting glucose and 24-hr blood pressure and not to metabolomics analyses. Thus, the combined Rifa-1 and Rifa-BP data set with $n = 34$ for fasting metabolomics and Rifa-2 data set with $n = 12$ for oral glucose tolerance test metabolomics present samples of convenience for the study of metabolome. The subjects visited the Internal Medicine Research Unit of Oulu University Hospital, Oulu, Finland as outpatients. After the first tablet was taken under the supervision of a study nurse, the participants were asked to take their daily doses at home between 4 and 8 p.m. at least 1 hour before and 2 hours after a meal. The details of the experimental protocols in Rifa-1 and Rifa-2 are described in the previous publications (Hukkanen, Rysä, et al., 2015; Rysä et al., 2013). In Rifa-2, the oral glucose tolerance test was performed on the morning of the first study day before rifampicin dosing and the second oral glucose tolerance test was performed on the morning of the eight study day. The oral glucose tolerance test time points were 0, 30, 60, 90 and 120 min. The Rifa-BP trial employed 24-hr ambulatory blood pressure measurements at the end of each 7-day rifampicin or placebo arm (Hassani-Nezhad-Gashti et al., 2020). In all three trials, the participants were asked to abstain from the use of alcohol, over-the-counter medications and dietary and herbal supplements during the study arms. Smoking and coffee drinking were allowed. The subjects consumed their regular diets during the study arms. In Rifa-BP trial, the subjects were also asked to abstain from the use of liquorice-containing products, salty snacks as well as energy drinks.

A written, informed consent was obtained from each study subject. The Ethics Committee of the Northern Ostrobothnia Hospital District (Oulu, Finland) (decision numbers 78/2009 for Rifa-1, 73/2010 for Rifa-2 and 6/2012 for Rifa-BP) and the Finnish Medicines Agency Fimea approved the studies. The study procedures were in accordance with the ethical standards of the Declaration of Helsinki and guidelines on Good Clinical Practice. The study subjects were financially compensated for participation. The trials were registered at ClinicalTrials.gov (Rifa-1 NCT00985270, Rifa-2 NCT01293422 and Rifa-BP NCT01690104).

2.2 | Analytical methods of human serum samples

A high-throughput nuclear magnetic resonance (NMR) metabolomics platform was used for the quantification of serum lipid and metabolite measures that represent a broad molecular signature of systemic

metabolism. The experimental setup allows for the simultaneous quantification of routine lipids, lipoprotein subclass distributions, fatty acids, as well as other low-molecular weight metabolites, such as amino acids and glycolysis-related metabolites and ketone bodies in absolute concentration units (Soininen et al., 2015). The spectroscopic and analytical characteristics of the platform have been detailed elsewhere (Inouye et al., 2010; Soininen et al., 2009; Würtz et al., 2016; Würtz & Soininen, 2020).

Serum 5α-cholest-7-en-3β-ol (lathosterol) concentration was measured in samples from Rifa-BP subjects by GCxGC-QTOFMS system (Pegasus 4D system, LECO; Saint Joseph; USA) with a method described previously (Castillo et al., 2011). Shortly, sample preparation was performed by adding 400 μl of methanol to 30 μl of serum samples to precipitate the proteins; after addition of internal standards (4βHC-D7, 25HCD6, desmosterol-D6 $c = 0.25$ mg·L^{-1}, heptadecanoic acid-d33 [175.36 mg·L^{-1}], valine-d8 [35.72 mg·L^{-1}], succinic acid-d4 [58.54 mg·L] and glutamic acid-d5 [110.43 mg·L^{-1}]) and after evaporation, the sample was derivatised with 25 μl of methoxyamine hydrochloride (60 min, 45°C) and with 40 μl of N-methyl-N-(trimethylsilyl)trifluoroacetamide (60 min, 45°C). Before injection, 50 μl of hexane was added to increase the volatility of the solvent. Additional standards here added during derivatization. n-Alkanes ($c = 8$ mg·L^{-1} in hexane) were used for calculation of retention indexes and 4,4′-dibromooctafluorobiphenyl ($c = 9.8$ mg·L^{-1} in hexane) was used as injection standard to control the quality of injection. Data were normalized with internal standards.

4-β-OH-cholesterol was measured in Rifa-1 with a gas chromatography–mass spectrometry method as published previously (Hukkanen, Puurunen et al., 2015) and in Rifa-BP with a liquid chromatography–electrospray–high-resolution mass spectrometry method as described (Hautajärvi et al., 2018).

ApoB48 serum level was measured with Human ApoB48 (Apolipoprotein B48) ELISA Kit (Elabscience) and PCSK9 serum level with Human PCSK9 ELISA kit (Abcam ab209884) according to manufacturers' protocols.

2.3 | Animal experiments

All experiments on animals were approved by the National Animal Experiment Board, Finland (license numbers ESAVI/6357/04.10.07/2014 and ESAVI/8240/04.10.07/2017), according to the EU directive 2010/63/EU. Mice were housed in individual cages with wood chips bedding under 12-hr light cycle in the Laboratory Animal Centre, University of Oulu, Oulu, with ad libitum water and food. Animal experiments or subsequent analyses were not blinded as the same researchers conducted the experiments and analyses. None of the analyses involved subjective scoring. Because the human studies did not suggest any major sex differences, only male mice were used to avoid unnecessary use of animals. Animal studies are reported in compliance with the ARRIVE guidelines (Percie du Sert et al., 2020) and with the recommendations made by the *British Journal of Pharmacology* (Lilley et al., 2020).

The 6-week-old, male, C57BL/6 N mice, from the colony of the Laboratory Animal Centre, University of Oulu, were fed regular chow (18% of calories from fat; approximate fatty acid profile [% of total fat]: 16% saturated, 23% monounsaturated, 61% polyunsaturated; Envigo td. 2018) or high-fat diet (60% calories from fat; approximate fatty acid profile [% of total fat]: 36% saturated, 41% monounsaturated, 23% polyunsaturated; Envigo td. 06414) for 15 weeks to induce obesity. After this feeding period, the high-fat diet-fed mice were allocated to three groups to yield as similar average weights for the groups as possible, but otherwise randomly. High-fat diet alone, high-fat diet vehicle and high-fat diet pregnenolone-16α-carbonitrile groups contained 9, 8 and 8 mice, respectively. To prepare for potential loss of animals one extra mouse was subjected to high-fat diet treatment. However, no animals were lost during the treatment resulting in slightly unequal group sizes. Chow group contained the other litter mates, 10 mice. Group sizes were determined based on our prior experience with similar mouse studies. Treatment groups were administered 50 mg·kg^{-1} of pregnenolone-16α-carbonitrile or vehicle (30% dimethyl sulfoxide in corn oil) by intraperitoneal injections for 4 days once a day. Mice were fasted 12 hr overnight, orally gavaged 2 g·kg^{-1} of glucose and anaesthetized with midazolam/fentanyl-fluanisone. Two hours after glucose administration mice were killed with carbon dioxide and EDTA-plasma and tissues were collected and snap-frozen in liquid nitrogen.

PXR knockout (PXR-KO) mouse experiments: The PXR-KO mouse line was generated as described earlier and kindly provided by Dr. Wen Xie, University of Pittsburgh (Xie et al., 2000). The original mouse strain in the C57BL/6 J background was backcrossed six times to C57BL/6 N strain to comply with the subtrain of the wild-type mouse used. The male PXR-KO mice were subjected to an identical experiment as described above for the wild-type mice except that the high-fat diet-feeding lasted for 18 weeks. Six mice were allocated per group, as the strong effect of pregnenolone-16α-carbonitrile seen in the wild-type mice enabled group size reduction without losing statistical power.

2.4 | Materials

Pregnenolone 16α-carbonitrile (PCN), dimethyl sulfoxide (DMSO) and corn oil were purchased from Sigma-Aldrich. Rifampicin was a product of Orion Inc., Espoo, Finland. See section 2.6. for the agents used in immunoblotting and ELISA. See sections 2.7 and 2.8 for reagents and kits used in RNA extraction, qPCR and RNA sequencing.

2.5 | Lipid and bile acid analyses of mouse plasma and liver

Plasma and liver cholesterol and non-cholesterol sterols, lanosterol, zymostenol, desmosterol and lathosterol, and squalene (cholesterol precursors), and campesterol, sitosterol and avenasterol (plant sterols), and cholestanol (5α-saturated derivative of cholesterol), were

analysed using gas–liquid chromatography (GLC) with a 50-m capillary column (Ultra 2, Agilent Technologies, Wilmington, DE) and flame ionization detection with 5α-cholestane as internal standard as described earlier (Miettinen et al., 1989). In case of the liver samples, they were carefully homogenized before saponification. The concentrations of the non-cholesterol sterols and squalene were adjusted to cholesterol of the same GLC run and expressed as ratios to cholesterol (102 μg·mg^{-1} of cholesterol) in order to enable their comparison between samples with different cholesterol levels.

Total bile acids from plasma were measured with Mouse Total Bile Acids Assay kit (Crystal Chem).

2.6 | Protein extraction, immunoblotting and ELISA

Mouse liver total proteins were extracted by homogenizing tissue pieces in lysis buffer (20-mM Tris-Cl, 150-mM NaCl, 1-mM EDTA, 1-mM EGTA, 1% Triton-X100, 2.5-mM sodium pyrophosphate, 1-mM β-glycerophosphate, 1-mM Na_3VO_4, pH 7.5) with Halt™ protease and phosphatase inhibitor cocktail (Thermo Fisher Scientific), 1-mM DTT and 50-mM NaF with TissueLyzer II (Qiagen) for 2 min. Homogenates were centrifuged at 16,000g for 20 min at $+4°C$. Protein concentration was determined with Bio-Rad Protein Assay.

Cytosolic and nuclear protein fractions were isolated by homogenizing 100 mg of mouse liver to 400 μl of 0.1-M phosphate buffer (pH 7.4; supplemented with Complete Protease Inhibitor Cocktail (Roche) with TissueLyser II for 2 min. Three hundred fifty microliters of homogenate was diluted with 650 μl of 0.1-M phosphate buffer (pH 7.4) and centrifuged 15,000g for 15 s at $+4°C$. The pellet was suspended to 400 μl of 10-mM HEPES, 10-mM KCl, 0.1-mM EDTA, 0.1-mM EGTA, pH 7.4, supplemented with Protease Inhibitor Cocktail and incubated on ice for 15 min. Twenty-five microliters of 10% Igepal was added and samples vortexed 15 s. Then, the samples were centrifuged 15,000g for 30 s at $+4°C$ and the supernatant was collected as cytosolic protein fraction. The pellet was further suspended to 50 μl of 20-mM HEPES, 0.4-M NaCl, 1-mM EDTA, 1-mM EGTA, pH 7.4, supplemented with Protease Inhibitor Cocktail. The suspensions were shaken 15 min at $+4°C$, after which the samples were centrifuged 15,000g for 10 min at $+4°C$. The supernatant was collected as the nuclear protein fraction. Protein concentrations from the fractions were determined with Bio-Rad Protein assay.

Liver microsomal fractions were isolated by homogenizing 100 mg of liver to 400 μl of 0.1-M phosphate buffer (pH 7.4) with Tissuelyser II (Qiagen). Homogenate was centrifuged for 30 min 10,000 rpm at $+4°C$. The supernatant was further centrifuged with Beckman Optima L-70 K ultracentrifuge 39,000 rpm for 60 min at $+4°C$. The pellet was suspended to 0.1-M phosphate buffer (pH 7.4) as the microsomal fraction. Protein content was determined with Bio-Rad protein assay.

Aliquots of 30 μg of total liver protein, 20 μg of nuclear protein fraction and 10 μg of microsomal protein were separated with SDS-PAGE and transferred to nitrocellulose membranes with Trans-Blot

Turbo RTA Mini Nitrocellulose Transfer Kit (Bio-Rad) and Trans-Blot-Turbo (Bio-Rad). Membranes were blocked with Amersham ECL Prime Blocking Agent (GE Healthcare). Immunoblotting was performed with rabbit polyclonal antibody to INSIG1 (Abcam ab70784, RRID: AB_1269181, 0.5 μg·ml^{-1}), rabbit polyclonal antibody to SREBP2 (Abcam ab30682, RRID:AB_779079, 0.4 μg·ml^{-1}), rabbit polyclonal to SREBP1 (Abcam ab28481, RRID:AB_778069, 0.5 μg·ml^{-1}), rabbit polyclonal antibody to HMGCR (Santa-Cruz sc-271595, RRID: AB_10650274, 1 μg·ml^{-1}), rabbit monoclonal antibody to 24-dehydrocholesterol reductase (DHCR24; Cell Signaling Technology #2033, RRID:AB_2091448, 1:1,000) and mouse monoclonal antibody to β-actin (Sigma Aldrich A1978, RRID:AB_476692, 0.04 μg·ml). All primary antibody incubations were done in 0.1% TBS-Tween overnight at $+4°C$. Membranes were incubated with IRDye®680RD goat anti-mouse (LI-COR 926-68070, RRID:AB_10956588, 0.04 μg·ml^{-1}) and IRDye®800CW goat anti-rabbit (LI-COR 926-32211, RRID: AB_621843, 0.04 μg·ml^{-1}) secondary antibodies in 0.1% TBS-Tween for 1 hr at room temperature. Membranes were imaged with Odyssey Fc (LI-COR). All immuno-related procedures involved comply with the editorial on immunoblotting and immunohistochemistry (Alexander et al., 2018).

Plasma PCSK9 levels were determined with Mouse PCSK9 ELISA kit (Abcam ab215538) according to manufacturer's protocol.

2.7 | RNA extraction and qPCR

Total RNA from liver was extracted with RNAzol RT reagent (Sigma) according to manufacturer's protocol. One microgram of total RNA was reverse transcribed to cDNA with RevertAid Reverse Transcriptase (Thermo scientific) using random hexamer primers according to manufacturer's protocol. cDNA samples were diluted 1/10 with H_2O. Quantitative PCR (qPCR) was performed with FastStart Universal SYBR Green Master Mix (Roche) in ABI 7300 thermal cycler (Applied Biosystems) or with PowerUp SYBR Green Master Mix (Thermo scientific) in QuantStudio 5 (Applied Biosystems). GAPDH and TBP were used as reference genes. All qPCR reactions were optimized with primer concentration to reach 95%–105% reaction efficiency. qPCR primers are listed in Table S2. mRNA fold changes were calculated with $2^{-\Delta CT}$ method where fold change $= 2^{-\Delta Ct\ sample}/2^{-\Delta Ct\ control\ sample}$.

2.8 | RNA sequencing

For liver RNA sequencing, three mice per group were randomly selected. Total liver RNA was DNase treated with RNase-Free DNase Set (Qiagen) coupled with RNeasy MinElute Cleanup kit (Qiagen). RNA concentration was determined with Qubit using Qubit RNA BR Assay kit (Thermo Fisher Scientific) and RNA integrity numbers with Agilent 2100 bioanalyzer using Agilent RNA 6000 Nano Kit. Ribosomal RNA was depleted, RNA fragmented and cDNA libraries prepared for sequencing with TruSeq Stranded Total RNA with

Ribo-Zero Gold kit (Illumina). The sequencing run was performed with NextSeq550 (Illumina).

Raw data analysis was done with Chipster software (Kallio et al., 2011; RRID:SCR_010939). The 75-bp paired-end reads obtained were aligned to mouse Ensembl reference genome GRCm38.92 with HISAT2 (RRID:SCR_015530) and reads per gene were counted with HTSeq (RRID:SCR_005514). Differentially expressed genes were determined with DESeq2 (RRID:SCR_015687) using Benjamini–Hochberg corrected adjusted p-value cut-off of <.05.

Pathway analyses were done with the Ingenuity Pathway Analysis software (Qiagen; RRID:SCR_008653) to determine the most enriched pathways and to predict upstream regulators associated with differentially expressed genes. For pathways and upstream regulators, p value of overlap was calculated using right-tailed Fisher's exact test.

The complete data sets are available at the NCBI's Gene Expression Omnibus (GEO; RRID:SCR_005012) database (accession number GSE136667). Gene expression profiling data comply with the MIAME (Minimum Information About a Microarray Experiment) standard.

2.9 | Data and statistical analysis

The data and statistical analysis comply with the recommendations on experimental design and analysis in pharmacology (Curtis et al., 2018).

The statistical computations of clinical trial data were carried out using IBM SPSS Statistics for Windows (IBM, Armonk, NY, USA; RRID:SCR_002865). GraphPad Prism (GraphPad Software, La Jolla, CA, USA; RRID:SCR_002798) was used to calculate AUCs of the metabolomics data with the trapezoidal method during the 2-hr oral glucose tolerance test in Rifa-2. The calculations of incremental AUCs had measurements performed in fasting state as a baseline. If the subtraction of the baseline from any subsequent oral glucose tolerance test time point resulted in a negative peak in incremental AUC calculation, it was subtracted from the positive peak area (net area calculation). The nonparametric Wilcoxon signed rank test was used to compare the study arms in combined Rifa-1 and Rifa-BP fasting data set and before and after rifampicin treatment in Rifa-2 oral glucose tolerance test data set. To control the false discovery rate in the fasting state metabolomics, the p values were corrected by the Benjamini–Hochberg procedure. The Hochberg correction was counted by SPSS Syntax with formula $p\tilde{}(n) = p(n); \ p\tilde{}(i) = \min(\tilde{}p(i + 1), \ (n/i) \ p(i)), \ i = (n - 1), \ ...,1$, where p $(1) \le p(2) \le ... \le p(n)$ is the number of variables. A p value of <.05 after the Benjamini–Hochberg procedure was considered statistically significant in the fasting state metabolomics. However, both nominal and corrected p values are reported. In Rifa-2 oral glucose tolerance test AUC data set with $n = 12$, a higher false discovery rate of 0.1 (10%) was utilized. Correlations were determined with Pearson's correlation coefficient using GraphPad Prism and considered significant when $p < .05$.

The statistical analyses of animal experiments were done with GraphPad Prism. Differences between two study groups were compared with Student's two-tailed t-test and multiple group comparisons with one-way ANOVA and Tukey's post hoc test when the p value of $F < .05$ and there was no significant variance inhomogeneity. Statistical differences were considered significant when $p < .05$.

2.10 | Nomenclature of targets and ligands

Key protein targets and ligands in this article are hyperlinked to corresponding entries in the IUPHAR/BPS Guide to PHARMACOLOGY http://www.guidetopharmacology.org and are permanently archived in the Concise Guide to PHARMACOLOGY 2019/20 (Alexander, Cidlowski, et al., 2019; Alexander, Fabbro, et al., 2019).

3 | RESULTS

3.1 | Rifampicin affects fasting serum metabolomics by increasing IDL and LDL cholesterol and markers of cholesterol synthesis in humans

To test the hypothesis that activation of PXR affects cholesterol homeostasis in humans *in vivo*, we utilized two clinical studies, Rifa-1 and Rifa-BP, designed to investigate cardiometabolic effects of rifampicin, a prototypical human PXR activator (Chen & Raymond, 2006). Thirty-four healthy volunteers were administered rifampicin or placebo daily for 1 week in a crossover setting and the serum samples were collected after 10-hr fasting. Rifampicin elevated serum 4-β-OH-cholesterol, a marker of PXR target CYP3A4 activity, in all study subjects indicating compliance with the rifampicin dosing regimen (Figure S1a).

Serum samples were analysed with an NMR metabolomics platform developed to assess systemic metabolism (Soininen et al., 2009; Würtz et al., 2017). The ratios of mean concentrations of all lipoprotein subclasses and their lipid components after the rifampicin study arm compared with the placebo study arm are presented in Figure 1. Absolute mean values of all the metabolites measured after both study arms and p-values are presented in Table S3. Rifampicin treatment increased the concentration of intermediate-density lipoprotein (IDL) and LDL particles, and further their total lipid, phospholipid and total, free and esterified cholesterol components significantly (adjusted $p < .05$) compared with the placebo (Figure 1). All sizes of LDL (large, medium and small) exhibited similar increases in their concentration and lipid components. Some additional alterations in the lipoprotein lipid contents were also detected, but these were marginal compared with the ones in the IDL and LDL fractions. Although chylomicrons and the largest very low-density lipoproteins (VLDL) were not statistically significantly affected, there was a trend towards a decrease in their concentrations (Figure 1). It should be noted that concentrations of these fractions are minuscule when compared with IDL, LDL and especially HDL (Figure S1b).

Among the additional serum NMR parameters, rifampicin study arm demonstrated significant increases in total cholesterol (from 3.7 to 4.0 mmol·L^{-1}), total cholesterol in LDL (from 1.2 to 1.4 mmol·L^{-1}), esterified and free cholesterol, whereas cholesterol in VLDL, remnant

FIGURE 1 Effect of rifampicin on human serum lipoprotein fractions. Lipoprotein parameters are expressed as ratios of mean concentration after the study arms (rifampicin/placebo; $n = 34$). The results with statistically significant difference by nominal P value ($P < .05$) are indicated by asterisk and after the Hochberg correction (adjusted $P < .05$) by double asterisk. Abbreviations: P, particle concentration; L, total lipids; PL, phospholipids; C, total cholesterol; CE, cholesterol esters; FC, free cholesterol; TG, triglycerides; VLDL, very low-density lipoprotein; IDL, intermediate-density lipoprotein; LDL, low-density lipoprotein; HDL, high-density lipoprotein; XXL, chylomicrons and extremely large; XL, very large; L, large; M, medium; S, small; XS, very small. See also Table S3 and Figure S1b
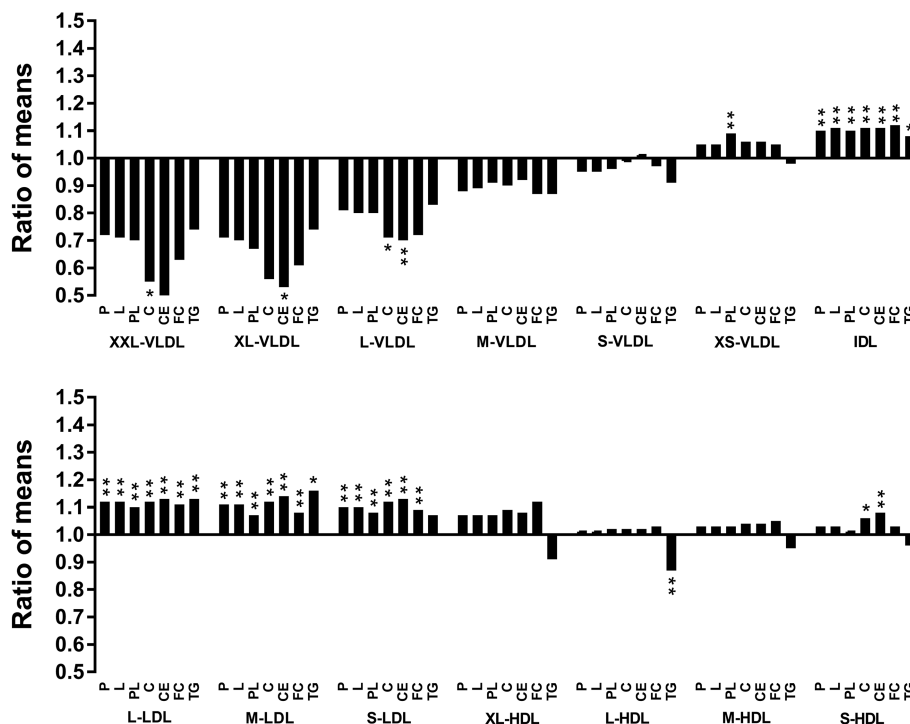
cholesterol (non-HDL-, non-LDL-cholesterol) and triglycerides were not affected (Figure 2a, Table S3). Total cholesterol in HDL and HDL2 was increased nominally significantly, but these effects did not retain statistical significance after correction for multiple testing. Interestingly, the changes in 4-β-OH-cholesterol correlated with the rifampicin-induced changes in serum total cholesterol ($r = 0.4688$), LDL-cholesterol ($r = 0.4458$), IDL ($r = 0.476$) and LDL particles ($r = 0.4551$) (Figure 3) indicating an association between PXR activation and serum lipid parameters. Moreover, rifampicin increased sphingomyelins, a possible risk marker for atherosclerosis and cardiovascular diseases (Figure 2a) (Fernandez et al., 2013). Atheroprotective apolipoprotein A1 (ApoA1) was increased whereas apolipoprotein B (ApoB) to ApoA1 ratio, a predictor of cardiac risk, was not affected (Ingelsson et al., 2007; Khuseyinova & Koenig, 2006). In addition, the total concentration of polyunsaturated omega-6 fatty acids was increased by rifampicin, due to an increase of linoleic acid.

Interestingly, serum concentrations of citrate and acetate, precursors of cholesterol and fatty acid synthesis, were decreased (Figure 2a), possibly due to increased cholesterol synthesis (Li et al., 2015; Yoshii et al., 2015). To further assess the effect of rifampicin on cholesterol synthesis, we determined the serum concentration of lathosterol, a cholesterol synthesis intermediate, from the Rifa-BP study samples. Rifampicin increased lathosterol to cholesterol ratio (Figure 2b), a surrogate marker for cholesterol synthesis (Björkhem et al., 1987).

In summary, the fasting serum metabolomics screen indicates that rifampicin increases serum IDL and LDL fractions. The increase of the synthesis intermediate lathosterol and decrease of cholesterol synthesis precursors, citrate and acetate, suggests that this effect is due to activation of cholesterol synthesis.

3.2 | Effect of rifampicin on cholesterol fractions during glucose challenge

Feeding may affect metabolic responses and a recent study utilizing metabolomics approach similar to this study reported the effect of glucose feeding (Wang et al., 2019). Moreover, we have reported the modifying effect of glucose feeding on PXR function in mouse liver (Hassani-Nezhad-Gashti et al., 2019). To analyse dynamics of the lipidome during glucose challenge in response to rifampicin, we utilized a third clinical study, Rifa-2, with oral glucose tolerance test (oral glucose tolerance test) in 12 healthy volunteers before and after 1-week rifampicin dosing.

According to the area under the curve (AUC) analysis, serum total cholesterol, total cholesterol in LDL and free cholesterol were elevated by rifampicin dosing (Figure S2, Table S4). The observed effect was mainly due to the increased concentration already at the 0 time point, reflecting the fasting response, and no further change was observed during the oral glucose tolerance test. Similarly, concentrations of IDL and all sizes of LDL particles were significantly increased as was their total lipid, phospholipid, cholesterol, free cholesterol and esterified cholesterol component concentrations (Table S4). Again, the effects were mainly due to the increased fasting levels and the incremental AUC values were not affected by rifampicin (Table S4).

Overall, the effect of rifampicin was quite similar in the Rifa-2 study during oral glucose tolerance test compared with the Rifa-1 and Rifa-BP studies (fasting). However, there were some important differences, the AUC of concentrations of very small VLDL particles and their total lipid, phospholipid, cholesterol, free cholesterol and esterified cholesterol components, were increased by rifampicin, whereas
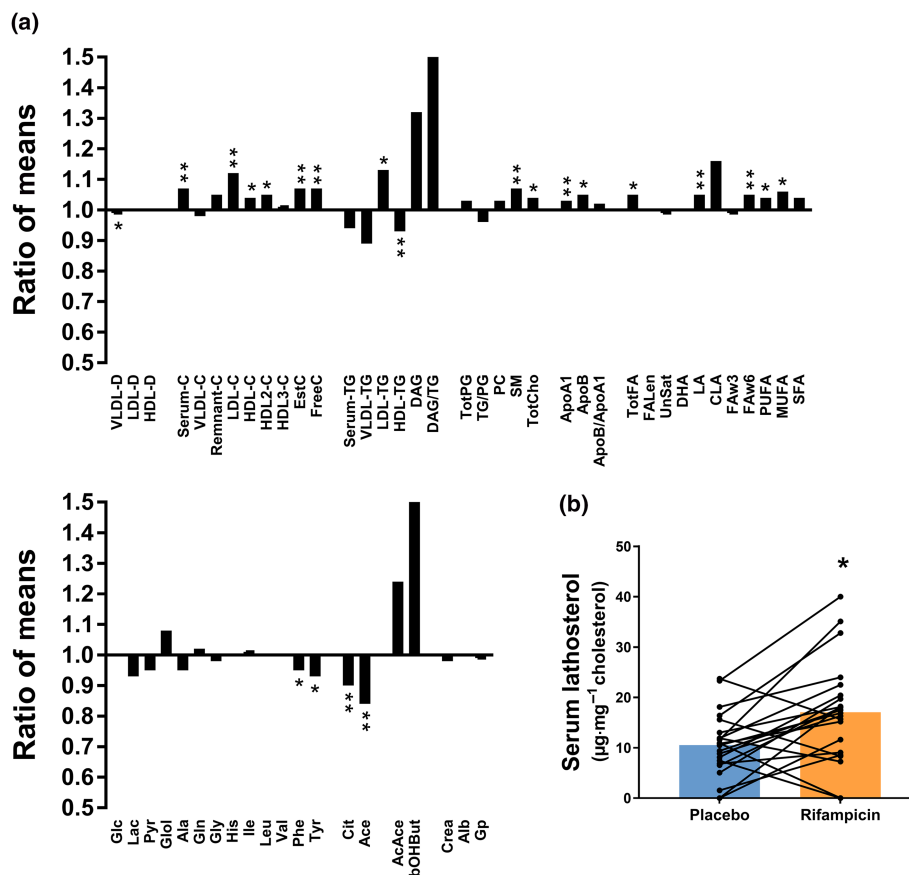
FIGURE 2 Effect of rifampicin on human serum lipid profile. (a) Lipid parameters are expressed as ratios of mean concentration after the study arms (rifampicin/placebo; n = 34). The results with statistically significant difference by nominal P value (P < .05) are indicated by asterisk and after the Hochberg correction (adjusted P < .05) by double asterisk. (b) Effect of rifampicin on lathosterol/cholesterol ratio (n = 18). *P < .05. Abbreviations: AcAce, acetoacetate; Ace, acetate; Ala, alanine; Alb, albumin; ApoA1, apolipoprotein A-I; ApoB, apolipoprotein B; bOHBut, 3-hydroxybutyrate; Cit, citrate; CLA, conjugated linoleic acid; Crea, creatinine; D, diameter; DAG, diacylglycerol; DHA, 22:6, docosahexaenoic acid; EstC, esterified cholesterol; FALen, estimated description of fatty acid chain length, not actual carbon number; FAw3, omega-3 fatty acids; FAw6, omega-6 fatty acids; Glc, glucose; Lac, lactate; Gln, glutamine; Glol, glycerol; Gly, glycine; Gp, glycoprotein acetyls, mainly a1-acid glycoprotein; His, histidine; Ile, isoleucine; LA, 18:2, linoleic acid; Leu, leucine; MUFA, monounsaturated fatty acids, 16:1, 18:1; PC, phosphatidylcholine and other cholines; PG, phosphoglycerides; Phe, phenylalanine; PUFA, polyunsaturated fatty acids; Pyr, pyruvate; SFA, saturated fatty acids; SM, sphingomyelins; TotCho, total cholines; TotFA, total fatty acids; Tyr, tyrosine; UnSat, estimated degree of unsaturation; Val, valine. See also Table S3

no changes were detected in the Rifa-1 and Rifa-BP studies. Also, AUC of remnant cholesterol was increased by rifampicin dosing (11% mean increase). Also notable was the increase in ApoB (mean increase 8%) and ratio of ApoB/ApoA AUCs after rifampicin. The serum concentration of ApoB48, the intestinal form of ApoB, was measured with ELISA to elucidate the role of intestine in the effect of rifampicin on ApoB. The fasting concentration and AUC of ApoB48 was significantly decreased by rifampicin dosing by 14% (2.5 ± 0.39 to 2.2 ± 0.51 μg·ml^{-1}) and 11% (284 ± 57 to 254 ± 57 min × μg·ml^{-1}), respectively (Figure S2b). Thus, the increase of total serum ApoB is possibly due to induced ApoB100 production in liver or altered kinetics of serum ApoB100.

The concentration of citrate decreased at the later oral glucose tolerance test timepoints in response to the rifampicin treatment (Figure S2a) suggesting rifampicin induced increase in the citrate consumption.

3.3 | Pregnenolone-16α-carbonitrile treatment induces cholesterol synthesis in the livers of obese mice

To identify the mechanisms mediating the activation of cholesterol synthesis by PXR ligands, we utilized a mouse model. Because the ligand-binding domains of human and mouse PXR differ significantly, different ligands need to be used for these two species (Kliewer et al., 2002). Pregnenolone-16α-carbonitrile is a prototypic rodent PXR ligand. In our previous studies, we have shown that 4-day pregnenolone-16α-carbonitrile treatment of mice on normal chow diet had no major effect on plasma cholesterol or the expression of the cholesterol biosynthesis genes in the liver (Hassani-Nezhad-Gashti et al., 2019). Indeed, mice on normal chow diet are rather resistant to changes in their lipid profile. Because dietary manipulation has
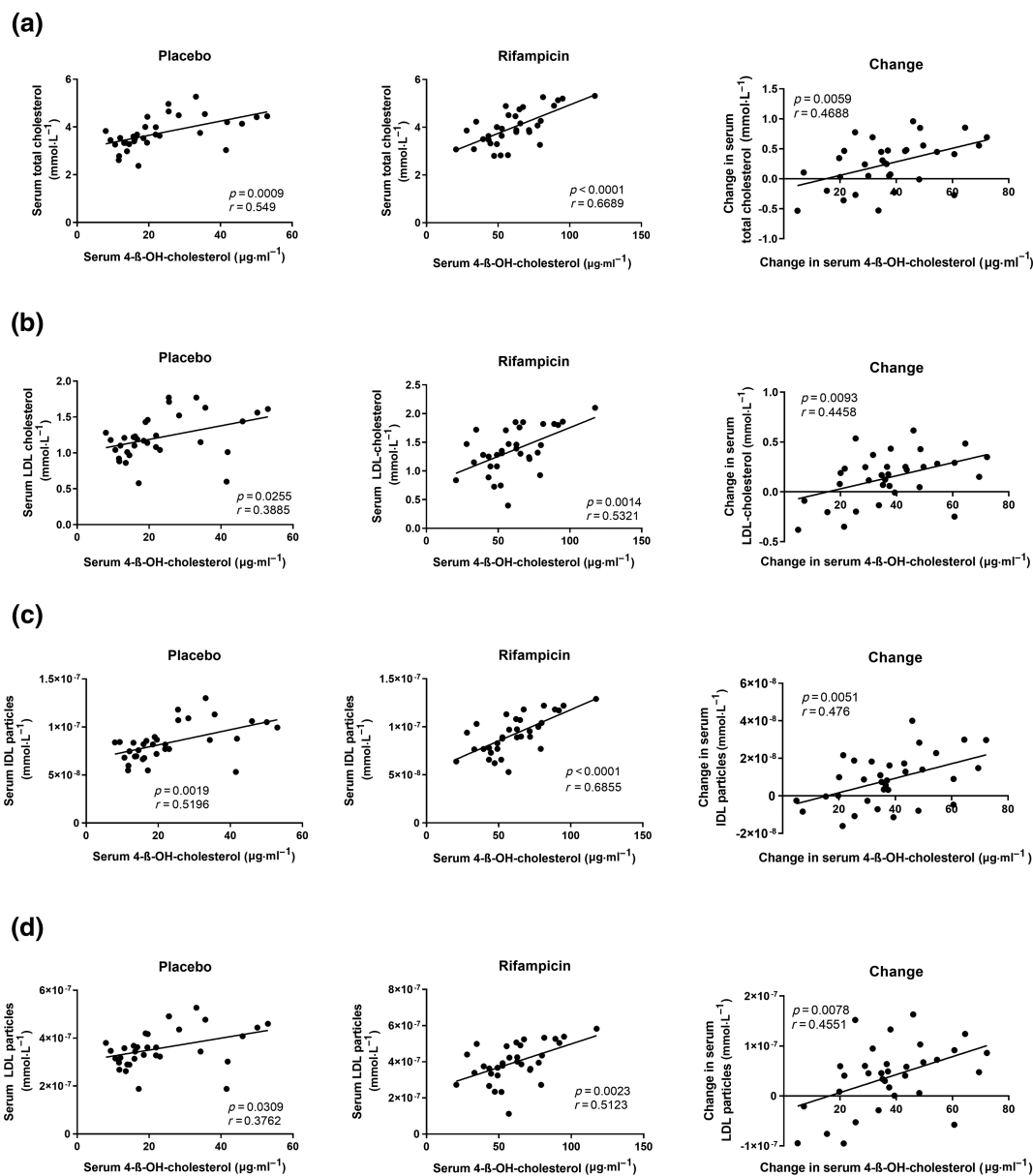
FIGURE 3 Serum 4-β-OH-cholesterol and rifampicin-induced changes in it correlate with cholesterol and lipoproteins. (a) Pearson correlation of 4-β-OH-cholesterol to total cholesterol. (b) Pearson correlation of 4-β-OH-cholesterol to LDL-cholesterol. (c) Pearson correlation of 4-β-OH-cholesterol to IDL particles. (d) Pearson correlation of 4-β-OH-cholesterol to LDL particles. The lines represent best fit by the linear regression. Correlations were considered statistically significant when $P < .05$

been proven to cause hypercholesterolemia in mice (Getz & Reardon, 2006), we hypothesized that high-fat diet challenge sensitizes the mice to PXR-induced hypercholesterolemia. Mice were subjected to high-fat diet feeding for 15 weeks to induce obesity and a subset was then treated with pregnenolone-16α-carbonitrile for 4 days.

As expected, high-fat diet increased plasma cholesterol compared with chow fed mice (Figure 4a). In addition, the liver cholesterol content was increased by the high-fat diet. Pregnenolone-16α-carbonitrile treatment had no effect on plasma cholesterol. In contrast, the liver cholesterol level was considerably higher in the pregnenolone-16α-carbonitrile-treated, high-fat diet-

fed mice compared with the vehicle-treated, high-fat diet-fed mice (Figure 4a).

To further investigate the origin of the increased liver cholesterol, we quantified markers of cholesterol synthesis (Figure 4b) in the plasma and liver and markers of cholesterol absorption in the plasma (Björkhem et al., 1987; Miettinen et al., 1989). In line with the human results, lathosterol to cholesterol ratio was increased both in the plasma and livers of the pregnenolone-16α-carbonitrile-treated mice (Figure 4c). Furthermore, zymostenol, another intermediate of the Kandutsch–Russell cholesterol synthesis pathway (Figure 4b), was strongly increased in the plasma and the liver (Figure 4c). By contrast, desmosterol, an intermediate of the Bloch pathway of cholesterol
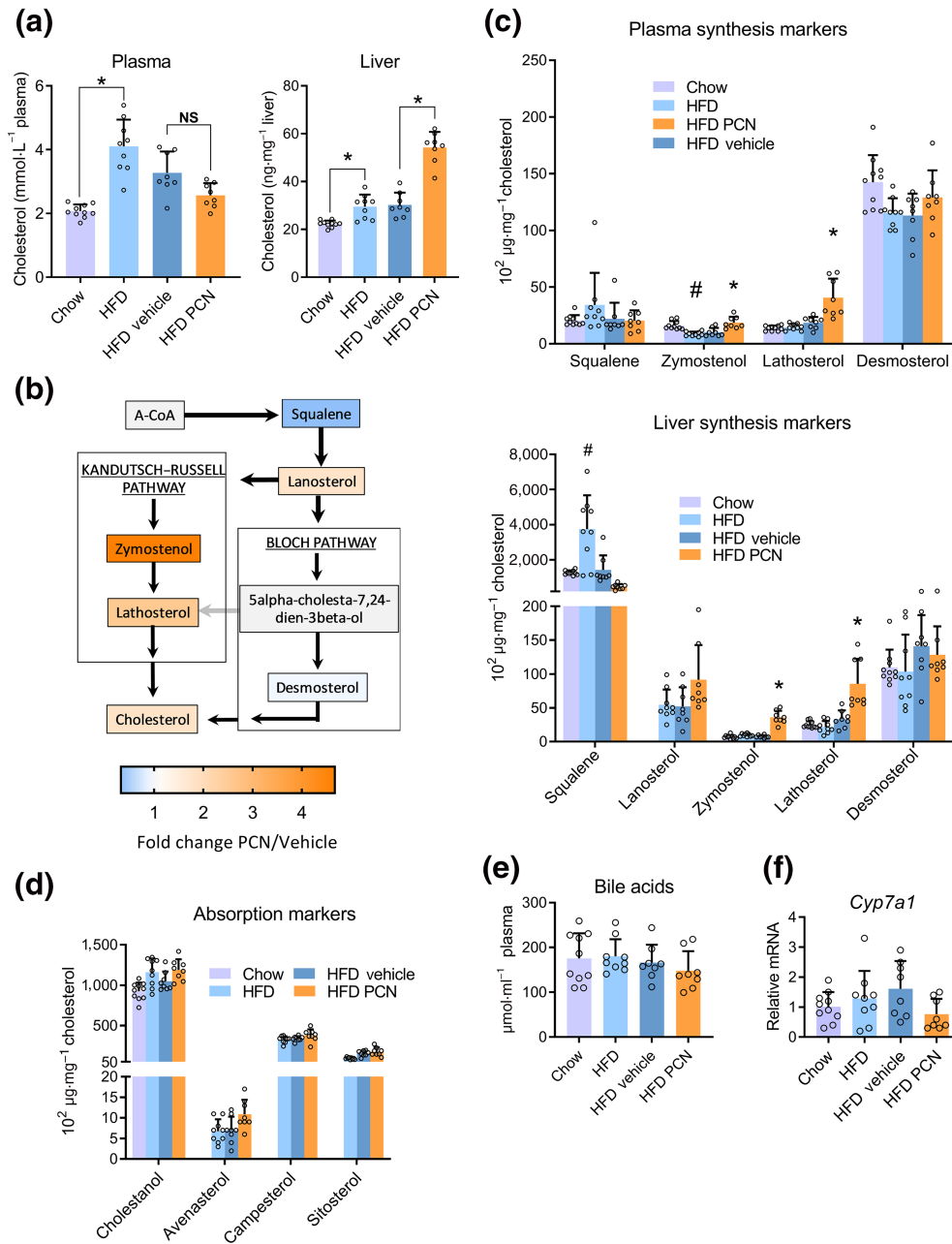
(a)

(b)

(c)

(d)

(e)

(f)

FIGURE 4 Pregnenolone-16α-carbonitrile (PCN) induces hepatic cholesterol synthesis in obese mice. (a) Cholesterol levels in plasma and liver. (b) Schematic diagram of hepatic cholesterol synthesis pathway and fold changes in synthesis intermediates. (c) Plasma and liver markers of cholesterol synthesis. (d) Markers of intestinal cholesterol absorption in mouse plasma. (e) Plasma total bile acids. (f) Liver *Cyp7a1* expression. Chow $n = 10$; high-fat diet (HFD) $n = 9$; HFD vehicle $n = 8$; HFD PCN $n = 8$. The values represent mean ± SD. Statistical difference to chow group marked with # and statistical difference to HFD vehicle group marked with *. */#$P < .05$

synthesis, was not affected by pregnenolone-16α-carbonitrile (Figure 4c). Plasma and liver squalene, an early intermediate of the cholesterol synthesis, was not significantly affected by pregnenolone-16α-carbonitrile (Figure 4b). Instead, the high-fat diet increased squalene level significantly in the liver but did not affect the Kandutsch–Russell cholesterol synthesis pathway intermediates (Figure 4c).

Cholesterol absorption markers, cholesterol metabolite cholestanol and the plant sterols avenasterol, campesterol and sitosterol, were not affected by pregnenolone-16α-carbonitrile treatment (Figure 4d) suggesting that pregnenolone-16α-carbonitrile has no effect on cholesterol absorption. A previous study reported that Niemann–Pick C1-like 1 (*Npc1l1*) and microsomal triglyceride transfer protein large subunit (*Mttp*) are intestinal PXR target genes, whose activation

leads to increased cholesterol absorption (Meng et al., 2019). In the current study, pregnenolone-16α-carbonitrile treatment increased the intestinal expression of *Cyp3a11* but did not affect *Npc1l1*, *Mttp* or *Apob* expression (Figure S3a,b). Instead, pregnenolone-16α-carbonitrile modestly induced *Abcb1a* and *Abcg5* involved in cholesterol excretion to the intestinal lumen (Figure S3c) (Temel & Brown, 2015).

Altogether, these results clearly indicate that the pregnenolone-16α-carbonitrile treatment induces hepatic cholesterol synthesis, especially the Kandutsch–Russell pathway, but has no increasing effect on cholesterol absorption.

Synthesis of bile acids represents a major route of cholesterol disposal. However, the high-fat diet did not affect total plasma bile acid

levels with or without pregnenolone-16α-carbonitrile treatment (Figure 4e). PXR has been reported to repress expression of **cholesterol 7 alpha-hydroxylase (CYP7A1)**, the rate-limiting enzyme of bile acid synthesis *in vitro* (Li & Chiang, 2005), but rifampicin dosing did not affect human hepatic CYP7A1 expression *in vivo* (Marschall et al., 2005). In the current experiment in the obese mice, pregnenolone-16α-carbonitrile treatment did not lead to statistically significant repression of *Cyp7a1* (Figure 4f). Furthermore, bile acids activate farnesoid X receptor (FXR), but the expression of hepatic FXR target genes was not altered by the pregnenolone-16α-carbonitrile treatment (Figure S4a).

The Bloch pathway intermediate desmosterol is a **liver X receptor** (LXR) ligand (Spann et al., 2012; Yang et al., 2006). In agreement with the lack of induction of the desmosterol levels by pregnenolone-16α-carbonitrile, the expression of hepatic LXR target genes was not altered in the liver (Figure S4b,c,d).

3.4 | PXR activation induces the superpathway of cholesterol biosynthesis in the livers of high-fat diet-fed mice

To further elucidate the mechanisms mediating the pregnenolone-16α-carbonitrile-elicited induction of cholesterol synthesis, three mice in each group were randomly selected for liver gene expression profiling by RNA sequencing. To explore the changes in the transcriptome, genes affected with adjusted *p* value < .05 were defined as differentially expressed genes in the RNA sequencing. Compared with the livers of the mice on regular chow, the high-fat diet alone differentially regulated 1,226 genes, of which 708 were upregulated and 518 downregulated. No cholesterol biosynthesis genes were among these genes.

The pregnenolone-16α-carbonitrile treatment of high-fat diet-fed mice differentially regulated 442 genes compared with the high-fat diet-vehicle mice, of which 276 were upregulated and 166 downregulated (Figure 5a, Table S5). To further characterize pathways affected by the pregnenolone-16α-carbonitrile treatment, we performed functional pathway enrichment analyses of differentially expressed genes with Ingenuity Pathway Analysis software (Krämer et al., 2014). The five most enriched pathways with the lowest *p* value of overlap are presented in the Figure 4b. Expectedly, the pathway *PXR/RXR activation* was among the top pathways (Figure 5b). The *Superpathway of cholesterol biosynthesis* was one of the top affected pathways supporting the significant effect of PXR activation on cholesterol synthesis (Figure 5b).

Detailed evaluation of the influence of pregnenolone-16α-carbonitrile on the *Superpathway of cholesterol biosynthesis* reveals a very drastic effect. Pregnenolone-16α-carbonitrile treated mice had higher expression level of almost all the genes involved in the cholesterol synthesis compared with only high-fat diet-fed or vehicle-treated groups (Figure 5c). One of the genes was HMG-CoA reductase (*Hmgcr*), the rate-limiting enzyme of cholesterol synthesis and the molecular target of statins. Figure 5d indicates the role of the

cholesterogenic enzymes in the cholesterol biosynthesis pathway and integrates the results of the RNA sequencing and the metabolite measurements.

The exploratory RNA sequencing findings were further confirmed with qPCR measurements of the full sample set. The cholesterol synthesis genes *Hmgcr*, *Fdps* and *Cyp51* as well as the well-established PXR target genes *Cyp3a11* and *Gsta1* were induced by pregnenolone-16α-carbonitrile (Figure 5e). To confirm the involvement of PXR in the pregnenolone-16α-carbonitrile-elicited induction of cholesterol synthesis, PXR-KO mice were subjected to similar treatment with high-fat diet and pregnenolone-16α-carbonitrile administration as described above for the wild-type mice. In the PXR-KO mice, pregnenolone-16α-carbonitrile had no effect on the expression of the cholesterol synthesis genes or the established PXR target genes (Figure 5e). Confirming the mRNA findings, pregnenolone-16α-carbonitrile increased microsomal **hydroxymethylglutaryl-CoA reductase HMGCR** protein level and the extent of protein induction was even higher, fourfold, than the mRNA induction (Figure 5f).

24-Dehydrocholesterol reductase is the bifurcation enzyme differentiating between the Kandutsch–Russell and Bloch pathways of cholesterol synthesis. The 24-dehydrocholesterol reductase protein was induced twofold by pregnenolone-16α-carbonitrile (Figure 5g) in accordance with the activation of the Kandutsch–Russell pathway.

3.5 | Pregnenolone-16α-carbonitrile treatment activates SREBP2 pathway in the liver

To further characterize the mechanisms mediating the induction of genes in the cholesterol biosynthesis pathway by PXR activation, we utilized Ingenuity Pathway Analysis software to predict the putative upstream regulators. The prediction of the upstream regulators of the 442 genes differentially regulated by pregnenolone-16α-carbonitrile is based on activation z-scores, which take into account the direction of gene expression, i.e., induction or repression.

As expected, PXR was among the most activated predicted upstream regulators (Figure 6a). Furthermore, the five most activated upstream regulators contained the master regulator of cholesterol synthesis, SREBP2 and SREBP cleavage activating protein (SCAP) (Figure 6a). The five most inhibited regulators contained insulin-induced gene 1 (INSIG1), which has a well-established role in inhibiting the cholesterol synthesis through repression of SREBP activity. Although in line with the induction of cholesterol synthesis, the inhibition of INSIG1 function is an unexpected prediction, because PXR has been previously shown to induce *Insig1* gene expression (A. Roth et al., 2008).

To validate the predictions of the upstream regulator analysis, we measured the mRNA expression of the *Srebp2* and the *Insig* in the wild-type and the PXR-KO mouse liver samples. The expression of *Srebp2*, *Insig2* or *Insig2a* was not affected by pregnenolone-16α-carbonitrile either in the wild-type or in the PXR-KO mice livers. In agreement with previous results (A. Roth et al., 2008), pregnenolone-16α-carbonitrile induced *Insig1* expression in the
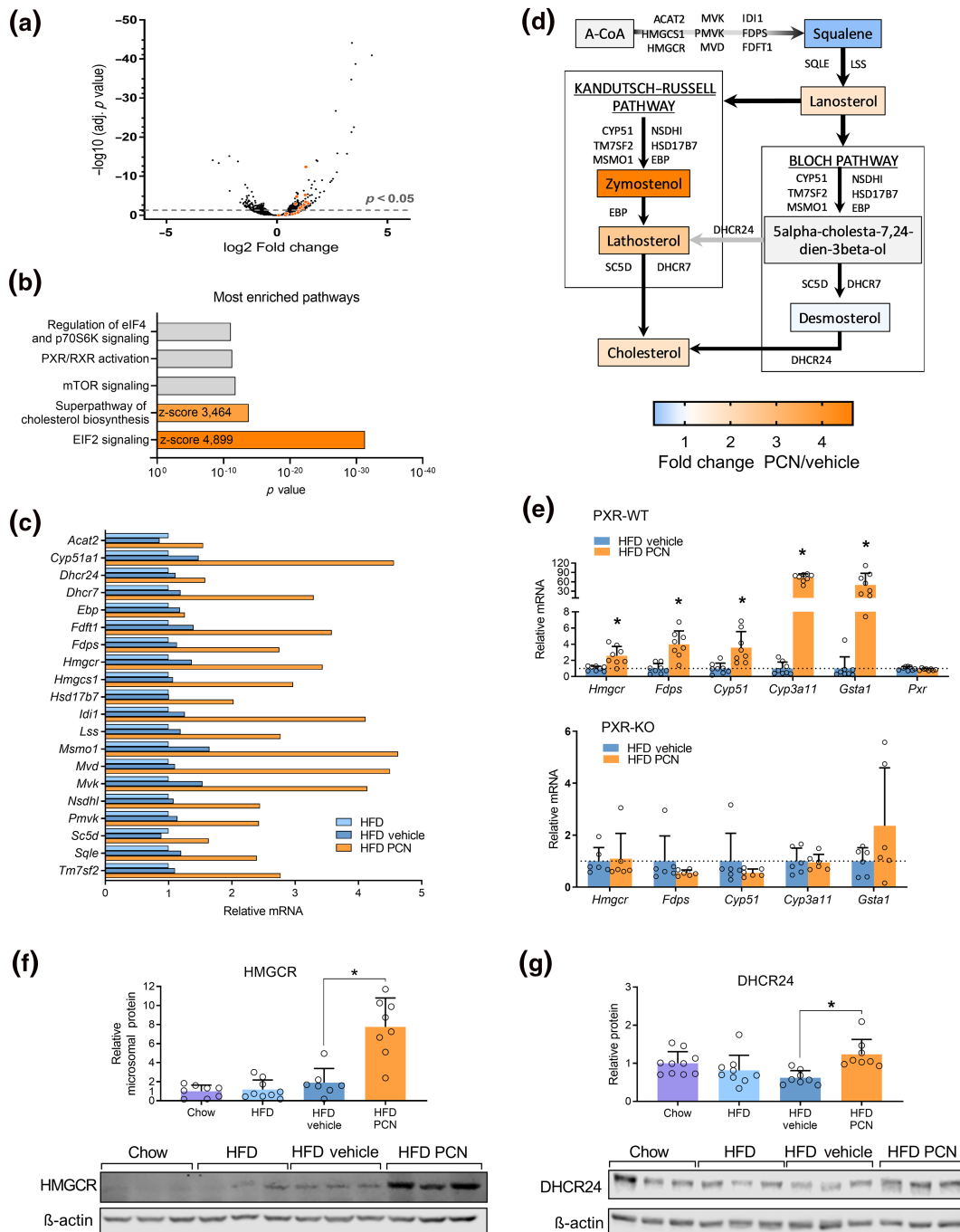
FIGURE 5 Pregnane X receptor (PXR) activation induces cholesterol biosynthesis pathway in the livers of obese mice. (a) Volcano plot of differentially expressed genes (276 up; 166 down) in the livers of high-fat diet (HFD)-fed and pregnenolone-16α-carbonitrile (PCN)-treated mice compared with vehicle control ($n = 3$/group). The cholesterol synthesis genes are indicated with orange dots. (b) Genes affected by PCN in RNAseq were allocated to biological pathways with Ingenuity Pathway Analysis software and activation z scores were calculated where it was possible. (c) Effect of PCN on cholesterol biosynthesis genes in RNASeq. Vehicle and PCN groups are compared with the HFD group ($n = 3$/group). No statistical analysis was performed. (d) Schematic diagram of hepatic cholesterol synthesis, fold changes of synthesis markers and genes involved in each step. (e) qPCR analysis of selected cholesterol biosynthesis genes and PXR target genes in PXR wild-type (PXR-WT; $n = 8$/group) and PXR knockout (PXR-KO; $n = 6$/group) mice. (f) Liver microsomal hydroxymethylglutaryl-CoA reductase (HMGCR) immunoblotting (chow $n = 8$; HFD $n = 9$; HFD vehicle $n = 7$; HFD PCN $n = 8$. Chow group lacked two samples and HFD vehicle group lacked one sample due to shortness of material. (g) Liver 24-dehydrocholesterol reductase (DHCR24) immunoblotting (chow $n = 10$; HFD $n = 9$; HFD vehicle $n = 8$; HFD PCN $n = 8$). The values (e–g) represent mean ± SD. *$P < .05$
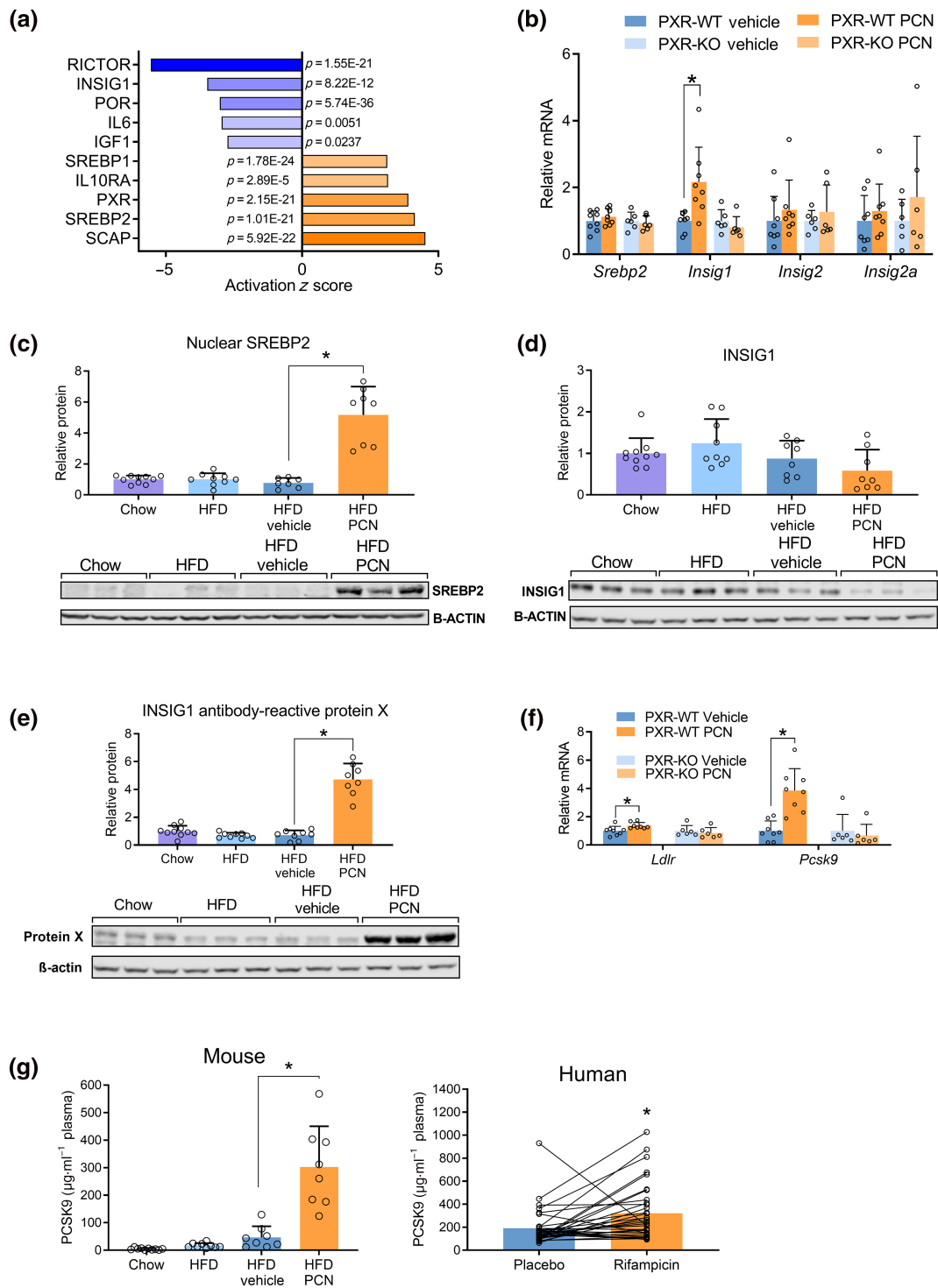
FIGURE 6 Pregnane X receptor (PXR) induces cholesterol synthesis and PCSK9 through the sterol regulatory element-binding protein 2 (SREBP2) pathway. (a) Top five upregulated and downregulated predicted liver upstream regulators in high-fat diet (HFD)-fed and pregnenolone-16α-carbonitrile (PCN)-treated mice compared with vehicle control based on liver RNAseq data, p values of overlap and activation z scores ($n = 3$/group). (b) Liver qPCR of cholesterol synthesis regulators in wild-type ($n = 8$/group) and PXR-KO mice ($n = 6$/group). (c) Immunoblotting of SREBP2 in the liver nuclear fraction (chow $n = 10$; HFD $n = 9$; HFD vehicle = 7; HFD PCN $n = 8$. HFD vehicle group lacked one sample due to shortness of material). (d) Immunoblotting of liver insulin-induced gene 1 (INSIG1) (chow $n = 10$; HFD $n = 9$; HFD vehicle $n = 8$; HFD PCN $n = 8$). (e) Immunoblotting of INSIG1-antibody-reactive protein X. (chow $n = 10$; HFD $n = 9$; HFD vehicle $n = 8$; HFD PCN $n = 8$). (f) qPCR measurement of *Ldlr* and *Pcsk9* mRNAs in the wild-type (PXR-WT; $n = 8$/group) and the PXR knockout (PXR-KO; $n = 6$/group) mice livers. (g) Effect of PXR ligands on the PCSK9 level in the mouse and the human plasma (mouse $n = 8$/group; human $n = 34$). The values represent mean ± SD. *$P < .05$

wild-type but not in the PXR-KO mice (Figure 6b). Therefore, the mRNA expression data did not support the Ingenuity Pathway Analysis software predictions of the upstream regulators.

Western blot analyses were performed to further clarify the activation status of the SREBP2 pathway. SREBP2 is activated through proteolytic processing in the Golgi and subsequent transport of the activated cleavage product to the nucleus (Shimano & Sato, 2017). Thus, the nuclear accumulation of SREBP2 reflects the activation of the pathway. Remarkably, the pregnenolone-16α-carbonitrile-treated mice had fivefold higher level of SREBP2 in the hepatic nuclear protein fraction than the vehicle control clearly indicating activation of the pathway (Figure 6c). Interestingly, the nuclear level of sterol regulatory element-binding protein 1 (SREBP1) or SREBP1 target genes were not induced by pregnenolone-16α-carbonitrile (Figure S5a,b).

INSIG1 promotes endoplasmic reticulum (ER) retention of SREBP2 thus inhibiting transfer to and activation in the Golgi. In the pregnenolone-16α-carbonitrile-treated mice, there was a tendency for a lower protein expression of INSIG1 (molecular weight 30 kDa), although the difference to the vehicle control was not statistically significant (Figure 6d). This data shows that transcriptional induction of *Insig1* mRNA by pregnenolone-16α-carbonitrile is not reflected to the functional protein level. Curiously, in the pregnenolone-16α-carbonitrile-treated mice samples, there was a much higher level of a larger size, 55-kDa protein (protein X) immunoreactive with the INSIG1 antibody (Figure 6e). The identity of this protein is currently unclear.

3.6 | PXR activation increases plasma PCSK9

Besides cholesterol synthesis genes, SREBP2 regulates genes involved in the hepatic LDL uptake: LDL receptor (*Ldlr*) and *Pcsk9* (Lagace, 2014). The LDLR mediates the hepatic uptake of LDL and PCSK9 is the major negative regulator of LDLR. Both *Ldlr* and *Pcsk9* mRNAs were induced by pregnenolone-16α-carbonitrile in the wild-type but not in the PXR-KO mice (Figure 6f) and especially *Pcsk9* was strongly induced, about fourfold. Moreover, pregnenolone-16α-carbonitrile increased mouse plasma PCSK9 more than sixfold compared with the vehicle-treated mice (Figure 6g).

To evaluate the translational significance of the PCSK9 finding, we measured the effect of rifampicin administration on PCSK9 serum levels in humans. Similar to the mice, PXR ligand induced the serum level of PCSK9 compared with the placebo arm of the study (Figure 6g).

3.7 | PXR deficiency alters the cholesterogenic gene response to high-fat diet

In agreement with the previous studies (Getz & Reardon, 2006), we observed an increase in the plasma cholesterol levels in response to high-fat diet. Because PXR deficiency was previously shown to protect mice from obesity and obesity-induced metabolic impairments

(He et al., 2013), we investigated the effect of PXR-KO on the cholesterol homeostasis in response to high-fat diet. In contrast to the previous studies (He et al., 2013; Spruiell et al., 2014), PXR deficiency did not protect against the high-fat diet-induced obesity and the weight gain was similar in the PXR-KO and the wild-type mice (Figure 7a).

High-fat diet repressed the classical PXR target gene *Cyp3a11* in the wild-type but not in the PXR-KO mice (Figure 7b) indicating that *Cyp3a11* repression by the high-fat diet involves PXR and that the high-fat diet modifies PXR function. In RNA sequencing, high-fat diet had a rather modest effect on cholesterogenic genes in the wild-type mice and none of the members of the superpathway of cholesterol biosynthesis were differentially regulated. However, in the qPCR measurements **farnesyl diphosphate synthetase gene (*Fdps*)** was induced about twofold (Figure 7b). The *Ldlr* was induced 1.6-fold, whereas the *Pcsk9* was not affected by the high-fat diet. Factors affecting SREBP2 signalling were not altered except *Insig2*, which was slightly repressed. Interestingly, in the PXR-KO mice the high-fat diet repressed *Srebp2*, *Insig1* and *Insig2a*, and SREBP2 target genes *Hmgcr*, *Cyp51* and *Pcsk9*. The *Fdps* and *Ldlr* induction, seen in the high-fat diet-fed wild-type mice, was abolished by the PXR deficiency (Figure 7b). Thus, PXR appears to be involved in the regulation of the SREBP2 pathway even in the absence of an exogenous ligand.

High-fat diet increased plasma PCSK9 level 3.7-fold in the wild-type mice. The PXR deficiency abolished the effect of high-fat diet, however the PCSK9 level was higher in the PXR-KO mice than in the wild-type mice (Figure 7c).

Because the high-fat diet feeding repressed *Srebp2* mRNA and its cholesterogenic target genes in the PXR-KO mice, we evaluated if the PXR deficiency affects the rise of the plasma cholesterol in response to high-fat diet. Plasma cholesterol was increased twofold in both the wild-type and the PXR-KO mice in response to the high-fat diet (Figure 7d) indicating that despite the effect of PXR-KO on the *Srebp2* and cholesterol synthesis genes, the PXR-KO could not prevent high-fat diet-induced increase in the plasma cholesterol.

4 | DISCUSSION

In the current study, we show that treatment with rifampicin, a human pregnane X receptor (PXR) ligand, raises serum IDL and LDL of all sizes and serum total, esterified and free cholesterol. Furthermore, rifampicin increases the lathosterol to cholesterol ratio suggesting upregulation of cholesterol synthesis. This harmful effect of rifampicin on serum parameters is compounded by increases in sphingomyelins and PCSK9, other risk factors for cardiovascular diseases (Schlitt et al., 2006; Seidah et al., 2014).

Previous studies in patients treated with PXR-activating drugs including several antiretroviral drugs and atypical antipsychotic quetiapine have shown increased cholesterol levels during treatment (de Leon et al., 2007; Estrada & Portilla, 2011). Furthermore, the antiepileptics with PXR-activating properties, that is, **phenytoin**, **phenobarbital** and **carbamazepine**, induce cholesterol levels, whereas **valproic acid** with no affinity to PXR does not (Eirís et al., 2000;

FIGURE 7 Cholesterol synthesis genes and Pcsk9 are repressed in the pregnane X receptor (PXR)-KO mice on high-fat diet. (a) Effect of high-fat diet (HFD) on weight gain and percentual weight gain in the wild-type (chow $n = 10$; HFD $n = 25$) and the PXR knockout mice (chow $n = 6$; HFD $n = 18$). (b) Effect of PXR deficiency on mRNA expression of PXR target genes and key genes controlling or being involved in cholesterol synthesis during HFD (WT, chow $n = 10$; HFD $n = 9$ and PXR-KO mice, $n = 6$/group). (c) Effect of HFD on plasma PCSK9 levels in the PXR-WT (chow $n = 10$; HFD $n = 9$) and the PXR-KO mice ($n = 6$/group). (d) Effect of HFD on plasma cholesterol levels in the PXR-WT (chow $n = 10$; HFD $n = 9$) and the PXR-KO ($n = 6$/group) mice. The values represent mean ± SD. *$P < .05$
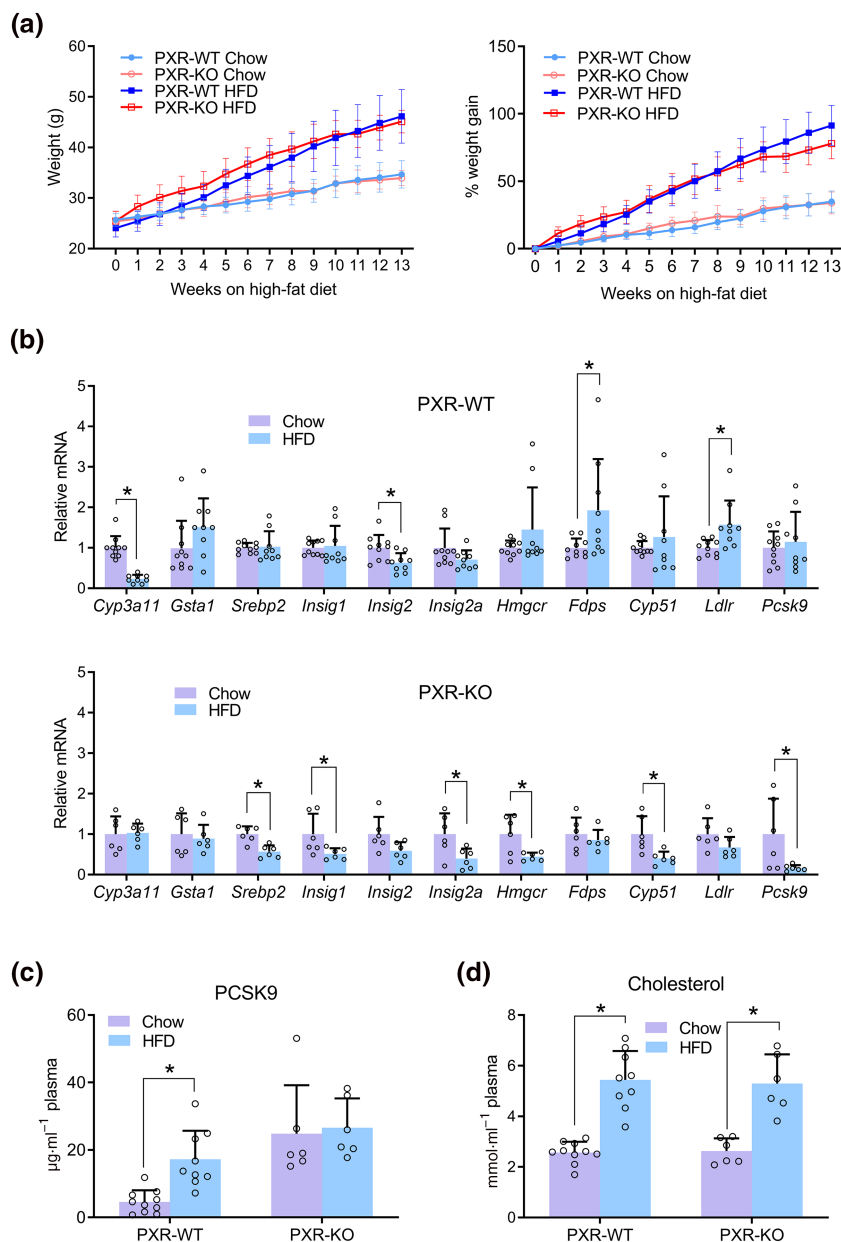
Luoma et al., 1979; Müjgan Aynaci et al., 2001). Importantly, phenobarbital induces human hepatic HMGCR protein *in vivo* (Coyne et al., 1976). Cafestol, a PXR ligand found in unfiltered coffee, raises blood cholesterol and is a risk factor for cardiovascular diseases (Ricketts et al., 2007; Weusten-Van der Wouw et al., 1994). Additionally, *PXR* gene polymorphisms associate with plasma LDL cholesterol levels in humans (Lu et al., 2010). Despite mounting epidemiological evidence linking PXR to cholesterol, the controlled human clinical studies are scarce.

Effect of rifampicin on cholesterol synthesis has previously been studied in one small clinical trial with ten healthy volunteers (Lütjohann et al., 2004). Although the serum total cholesterol level was not affected, rifampicin treatment increased the lathosterol to cholesterol ratio suggesting increase in cholesterol synthesis in

agreement with our current study. Furthermore, a study with daily cholesterol measurement for 30 days reported that 14-day rifampicin dosing led to 9.5% increase in total cholesterol with gradual decrease to baseline after stopping the treatment (Kasichayanula et al., 2014). The effect was not statistically significant due to small sample size ($n = 12$) but it resembles our result (7% increase). A few small studies have observed no change in total cholesterol during rifampicin treatment (Feely et al., 1983; Ohnhaus et al., 1979). Our studies form the largest clinical study set investigating the effect of rifampicin on cholesterol homeostasis and the only one reporting systemic metabolomic changes.

Rifa-1 and Rifa-BP studies utilized in the current investigation had identical crossover setting. The oral glucose tolerance test study (Rifa-2) had a one-arm design with oral glucose tolerance test

performed before and after 1-week rifampicin dosing. All three studies were performed on healthy young individuals with no overlapping medications or confounding illnesses. The metabolomic screen was systematic in nature and differences were first and foremost seen in the cholesterol metabolism, as for example triglyceride levels remained unaltered. In agreement with the hypothesis that the changes in serum cholesterol by rifampicin are PXR dependent, serum 4-β-OH-cholesterol, a marker of PXR activation (Diczfalusy et al., 2009), correlated with increases in serum total cholesterol.

Cholesterol in the blood originates from either the diet through intestinal absorption or from *de novo* synthesis occurring mostly in the liver. Rifampicin decreased citrate and acetate consumed in cholesterol synthesis and increased lathosterol to cholesterol ratio, an indicator of cholesterol synthesis suggesting that rifampicin mainly affects cholesterol biosynthesis. Although citrate and acetate are also consumed in other metabolic, PXR-regulated pathways such as fatty acid synthesis, lathosterol is a well-established marker of cholesterol synthesis (Björkhem et al., 1987; Hakkola et al., 2016). The levels of remnant cholesterol and ApoB were significantly elevated by rifampicin only in the Rifa-2 study. The elevation of ApoB (the protein component of VLDL, IDL and LDL) is of importance because cholesterol is secreted from the liver in VLDL particles that are metabolized to IDL and further to LDL (Laufs et al., 2019).

The fraction containing chylomicrons (chylomicrons and extremely large VLDL particles) derived from intestine trended numerically towards a decrease. The decrease of intestinally produced ApoB48 in serum suggests that the intestinal cholesterol absorption and chylomicron assembly is repressed by PXR activation. This supports the notion that intestinal absorption and synthesis of cholesterol do not play a role in the PXR-induced increase in serum cholesterol. Indeed, using high-fat diet-fed mouse as a model, we established that PXR activation causes induction of hepatic cholesterol synthesis, but it does not enhance cholesterol absorption.

Previously, one cholesterol biosynthesis gene, squalene epoxidase (*Sqle*), was shown to be a direct PXR target (Gwag et al., 2019). In the current study, we observed widespread induction of the genes in the cholesterol synthesis superpathway. Experiments in the PXR-KO mouse indicated that PXR was necessary for the pregnenolone-16α-carbonitrile-mediated induction of the cholesterol synthesis genes. Although not formally excluded, we consider it unlikely that all the cholesterol synthesis genes upregulated by pregnenolone-16α-carbonitrile would be direct PXR targets. Instead, we observed activation of SREBP2, a master regulator of the cholesterol synthesis (Shimano & Sato, 2017).

The mRNA expression of *Srebp2* was not affected by PXR activation. Indeed, the protein processing is the major step controlling SREBP2 activity. SREBP2 transcriptional activity requires processing in Golgi and proteolytic release of the active fragment entering nucleus. INSIG1 is an endoplasmic reticulum (ER)-retention membrane protein hindering SREBP2 transfer to Golgi. Sterol level regulates INSIG1 stability and subsequently SREBP2 transfer and processing. In a situation of low sterol content, INSIG1 is degraded while SREBP2 is cleaved and translocated to the nucleus to induce

its target genes (Shimano & Sato, 2017). Interestingly, even when the liver cholesterol level was high in the pregnenolone-16α-carbonitrile-treated mice livers, the SREBP2 was activated indicating interference of the normal regulation of the SREBP2 pathway. This appears to be at least partially mediated through INSIG1. In the presence of high liver cholesterol INSIG1, protein is expected to be stabilized. By contrast, the INSIG1 level tended to be lower in the pregnenolone-16α-carbonitrile-treated mice livers. The lower INSIG1 protein level after pregnenolone-16α-carbonitrile treatment also contrasts with the induction of the *Insig1* mRNA. These results suggest that PXR may affect the proteolytic machinery controlling INSIG1 stability.

In addition to regulating SREBP2 function, INSIG1 plays a role in the regulation of HMGCR protein stability and in the presence of high cholesterol, INSIG1 promotes HMGCR degradation (Sever et al., 2003). However, in our experiments, the *Hmgcr* mRNA was induced 2.6-fold and the HMGCR protein fourfold by the pregnenolone-16α-carbonitrile treatment suggesting protein stabilization of HMGCR despite the high cholesterol, again supporting the concept of altered INSIG1 function.

A Bloch pathway intermediate desmosterol acts as a negative feedback regulator in the cholesterol synthesis by inhibiting the SREBP2 processing (Spann et al., 2012; Yang et al., 2006). Interestingly, we observed a shift towards Kandutsch–Russell pathway and no change in the desmosterol levels. This mechanism may also contribute to the lack of SREBP2 inhibition.

Another key finding of the current study is the increase in the circulating PCSK9 after PXR activation. Indeed, the same effect could be observed both in the mice and humans. It should be noted as a limitation to the study that the circulating PCSK9 level was measured in the mouse samples 2 hr after glucose treatment while the human measurements were made after fasting; however, the results were still in agreement. SREBP2 is the major regulator of *Pcsk9* gene and the upregulation of *Pcsk9* expression further substantiates the role of SREBP2 in the PXR-induced effects on cholesterol homeostasis (Lagace, 2014). The similar finding in the mice and humans supports the hypothesis that the SREBP2 pathway mediates the PXR-elicited alterations on cholesterol homeostasis in humans, too.

PCSK9 has been proven a very important player in cholesterol homeostasis. PCSK9 is strongly linked to the levels of LDL-cholesterol and to the incidence of cardiovascular diseases (Seidah et al., 2014). Therefore, it is plausible that together with the increased cholesterol synthesis, also the impaired hepatic LDL uptake due to increased PCSK9 contributes to the elevated LDL cholesterol. Figure 8 summarizes the mechanisms revealed in the current study and mediating the effect of PXR activation on cholesterol and lipoprotein homeostasis.

Statins decrease intracellular cholesterol content and, in response, activate SREBP2 to induce PCSK9 levels in the plasma. To fight against this harmful compensatory mechanism, drugs inhibiting PCSK9 are used to treat hypercholesterolemia in combination with statins (Seidah et al., 2014; Warden et al., 2019). A recent meta-analysis reported that lipophilic statins (**atorvastatin**, **simvastatin**) elevate PCSK9 levels more than hydrophilic statins (**rosuvastatin**, **pravastatin**)
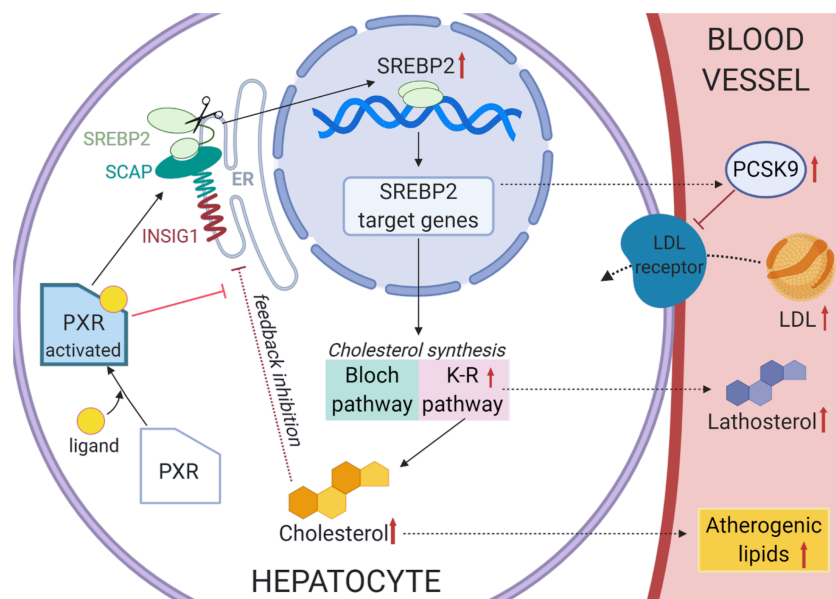
FIGURE 8   Mechanism of pregnane X receptor (PXR) mediated regulation of cholesterol and lipoprotein homeostasis. PXR activation promotes sterol regulatory element-binding protein 2 (SREBP2) proteolytic activation resulting in transcriptional activation of SREBP2 target genes: (1) widespread induction of cholesterol synthesis genes including the rate limiting *Hmgcr* and (2) *Pcsk9*, regulating the amount of LDL receptor in the hepatocyte plasma membrane. PXR activation increases cholesterol synthesis through the Kandutsch–Russell pathway and not through the Bloch pathway. While increase of the cholesterol synthesis is expected to launch feedback inhibition through insulin-induced gene 1 (INSIG)-mediated inhibition of SREBP2 proteolytic activation, this negative feedback pathway appears not to function under PXR activation. Altogether, these mechanisms result in increased level of atherogenic lipids

(Sahebkar et al., 2015). Because the lipophilic statins activate PXR (Howe et al., 2011), it can be speculated that PXR plays a role in the greater PCSK9 induction potential of the lipophilic statins. Rifampicin now joins the very short list of drugs known to elevate PCSK9 (statins and fibrates) with rifampicin being the most efficient (about 1.7-fold PCSK9 elevation) (Glerup et al., 2017). Several other drugs used in long-term treatments are PXR ligands (Hukkanen, 2012). Whether these PXR-activating drugs induce PCSK9 plasma levels in the clinical practice requires further investigation.

We also assessed the effect of PXR deficiency on high-fat diet-induced hypercholesterolemia and on the cholesterogenic mechanisms. Contrary to the previous reports (He et al., 2013; Spruiell et al., 2014), PXR deficiency did not protect against the high-fat diet-induced obesity. The reason for this discrepancy is unknown but may be related to mouse strains. The previous studies were performed in the C57BL/6 J strain, but we utilized the C57BL/6 N background instead. The two strains differ by a mutation in the NAD(P) trans-hydrogenase gene affecting glucose homeostasis (Toye et al., 2005) and they differ in weight gain during high-fat diet (Nicholson et al., 2010). Nevertheless, the unaltered weight gain allowed us to directly assess the effect of PXR deficiency on cholesterol metabolism without the confounding effect of the weight.

Although both high-fat diet alone and the pregnenolone-16α-carbonitrile treatment in the high-fat diet background increased cholesterol synthesis in the wild-type mice, the mechanisms appear to be different. The high-fat diet treatment induced the liver squalene level,

whereas the pregnenolone-16α-carbonitrile treatment tended to decrease squalene. Furthermore, pregnenolone-16α-carbonitrile activated the Kandutsch–Russell cholesterol synthesis pathway, whereas high-fat diet alone did not. Importantly, high-fat diet did not increase HMGCR protein level or the nuclear SREBP2, although pregnenolone-16α-carbonitrile combined with high-fat diet stimulated strong induction of both. Curiously, the PXR-KO modified the gene response to high-fat diet. The induction of *Fdps* and *Ldlr* by high-fat diet was abolished; the mRNAs of *Srebp2* as well as SREBP2 target genes *Hmgcr*, *Cyp51* and *Pcsk9* were repressed. These findings indicate that even in the absence of any exogenous ligand, PXR modulates the SREBP2 pathway. PXR deficiency abolished the high-fat diet-induced upregulation of plasma PCSK9 but was not sufficient to prevent upregulation of plasma cholesterol level suggesting that PXR inhibition may not be a viable approach to prevent diet-induced hypercholesterolemia.

In summary, we show for the first time in controlled clinical studies that PXR activation induces cholesterol synthesis and elevates LDL and total cholesterol in humans. In addition, we report that PXR activation increases circulating PCSK9. On the basis of the experimentation in murine models, we propose that PXR induces hepatic cholesterol biosynthesis and *Pcsk9* expression through activation of SREBP2 by enhancing its proteolytic processing. Altogether, these results reveal a novel mechanism controlling human cholesterol and lipoprotein homeostasis and establish a molecular mechanism for drug-induced hypercholesterolemia.

ACKNOWLEDGEMENTS

AUTHOR CONTRIBUTIONS

Conceptualization: J.Hu., J.Ha., M.K. and M.J.S.; methodology: M.K., O.K., J.Hu., J.Ha., M.A.-K., H.H. and A.T.; investigation: M.K., A.J.K., J.Hu., O.K., H.G., T.H., M.O. and H.H.; formal analysis: M.K. and A.J.K.; writing – original draft: M.K., J.Ha., J.Hu. and A.J.K.; writing – review & editing: All authors; supervision: J.Hu. and J.Ha.

CONFLICT OF INTEREST

Ari Tolonen and Heidi Hautajärvi are employees and shareholders of Admescope Ltd. The other authors declare no competing interests.

DECLARATION OF TRANSPARENCY AND SCIENTIFIC RIGOUR

The paper adheres to the principles for transparent reporting and scientific rigour of preclinical research as stated in the *BJP* guidelines for Design & Analysis, Immunoblotting and Immunochemistry and Animal Experimentation, and as recommended by funding agencies, publishers and other organizations engaged with supporting research.

DATA AVAILABILITY STATEMENT

The complete RNA sequencing data sets are available at the NCBI's Gene Expression Omnibus (GEO) database with accession number GSE136667. The other data that support the findings of this study are available from the corresponding author upon reasonable request. Some data may not be made available because of privacy or ethical restrictions.

ORCID

Mikko Karpale https://orcid.org/0000-0002-4795-7729
Janne Hukkanen https://orcid.org/0000-0003-4981-0525
Jukka Hakkola https://orcid.org/0000-0001-5048-4363

REFERENCES

Alexander, S. P. H., Cidlowski, J. A., Kelly, E., Mathie, A., Peters, J. A., Veale, E. L., Armstrong, J. F., Faccenda, E., Harding, S. D., Pawson, A. J., Sharman, J. L., & Young, M. (2019). The Concise Guide to PHARMACOLOGY 2019/20: Nuclear hormone receptors. *British Journal of Pharmacology*, *176*, S229–S246.

Alexander, S. P. H., Fabbro, D., Kelly, E., Mathie, A., Peters, J. A., Veale, E. L., Armstrong, J. F., Faccenda, E., Harding, S. D., Pawson, A. J., Sharman, J. L., & Watts, V. (2019). The Concise Guide to PHARMACOLOGY 2019/20: Enzymes. *British Journal of Pharmacology*, *176*, S297–S396.

Alexander, S. P. H., Roberts, R. E., Broughton, B. R. S., Sobey, C. G., George, C. H., Stanford, S. C., Cirino, G., Docherty, J. R., Giembycz, M. A., Hoyer, D., Insel, P. A., Izzo, A. A., Ji, Y., MacEwan, D. J., Mangum, J., Wonnacott, S., & Ahluwalia, A. (2018). Goals and practicalities of immunoblotting and immunohistochemistry: A guide for submission to the *British Journal of Pharmacology*. *British Journal of Pharmacology*, *175*, 407–411. https://doi.org/10.1111/bph.14112

Bitter, A., Rümmele, P., Klein, K., Kandel, B. A., Rieger, J. K., Nüssler, A. K., Zanger, U. M., Trauner, M., Schwab, M., & Burk, O. (2015). Pregnane X receptor activation and silencing promote steatosis of human hepatic cells by distinct lipogenic mechanisms. *Archives of Toxicology*, *89*, 2089–2103. https://doi.org/10.1007/s00204-014-1348-x

Björkhem, I., Miettinen, T., Reihnér, E., Ewerth, S., Angelin, B., & Einarsson, K. (1987). Correlation between serum levels of some cholesterol precursors and activity of HMG-CoA reductase in human liver. *Journal of Lipid Research*, *28*, 1137–1143. https://doi.org/10.1016/S0022-2275(20)38603-X

Castillo, S., Mattila, I., Miettinen, J., Orešič, M., & Hyötyläinen, T. (2011). Data analysis tool for comprehensive two-dimensional gas chromatography/time-of-flight mass spectrometry. *Analytical Chemistry*, *83*, 3058–3067. https://doi.org/10.1021/ac103308x

Chen, J., & Raymond, K. (2006). Roles of rifampicin in drug-drug interactions: Underlying molecular mechanisms involving the nuclear pregnane X receptor. *Annals of Clinical Microbiology and Antimicrobials*, *5*, 3. https://doi.org/10.1186/1476-0711-5-3

Coyne, M. J., Bonorris, G. G., Goldstein, L. I., & Schoenfield, L. J. (1976). Effect of chenodeoxycholic acid and phenobarbital on the rate-limiting enzymes of hepatic cholesterol and bile acid synthesis in patients with gallstones. *The Journal of Laboratory and Clinical Medicine*, *87*, 281–291.

Curtis, M. J., Alexander, S., Cirino, G., Docherty, J. R., George, C. H., Giembycz, M. A., Hoyer, D., Insel, P. A., Izzo, A. A., Ji, Y., & Ahluwalia, A. (2018). Experimental design and analysis and their reporting II: Updated and simplified guidance for authors and peer reviewers. *British Journal of Pharmacology*, *175*, 987–993. https://doi.org/10.1111/bph.14153

de Leon, J., Susce, M. T., Johnson, M., Hardin, M., Pointer, L., Ruaño, G., Windemuth, A., & Diaz, F. J. (2007). A clinical study of the association of antipsychotics with hyperlipidemia. *Schizophrenia Research*, *92*, 95–102. https://doi.org/10.1016/j.schres.2007.01.015

Diczfalusy, U., Kanebratt, K. P., Bredberg, E., Andersson, T. B., Böttiger, Y., & Bertilsson, L. (2009). 4β-Hydroxycholesterol as an endogenous marker for CYP3A4/5 activity. Stability and half-life of elimination after induction with rifampicin. *British Journal of Clinical Pharmacology*, *67*, 38–43.

Eirís, J., Novo-Rodríguez, M. I., Del Río, M., Meseguer, P., Del Río, M. C., & Castro-Gago, M. (2000). The effects on lipid and apolipoprotein serum levels of long-term carbamazepine, valproic acid and phenobarbital therapy in children with epilepsy. *Epilepsy Research*, *41*, 1–7. https://doi.org/10.1016/S0920-1211(00)00119-4

Estrada, V., & Portilla, J. (2011). Dyslipidemia related to antiretroviral therapy. *AIDS Reviews*, *13*, 49–56.

Feely, J., Clee, M., Pereira, L., & Guy, E. (1983). Enzyme induction with rifampicin: Lipoproteins and drug binding to alpha 1-acid glycoprotein. *British Journal of Clinical Pharmacology*, *16*, 195–197. https://doi.org/10.1111/j.1365-2125.1983.tb04986.x

Fernandez, C., Sandin, M., Sampaio, J. L., Almgren, P., Narkiewicz, K., Hoffmann, M., Hedner, T., Wahlstrand, B., Simons, K., Shevchenko, A., James, P., & Melander, O. (2013). Plasma lipid composition and risk of

developing cardiovascular disease. *PLoS ONE*, *8*, e71846. https://doi.org/10.1371/journal.pone.0071846

Garg, A., & Simha, V. (2007). Update on dyslipidemia. *The Journal of Clinical Endocrinology & Metabolism*, *92*, 1581–1589. https://doi.org/10.1210/jc.2007-0275

Getz, G. S., & Reardon, C. A. (2006). Diet and murine atherosclerosis. *Arteriosclerosis, Thrombosis, and Vascular Biology*, *26*, 242–249. https://doi.org/10.1161/01.ATV.0000201071.49029.17

Glerup, S., Schulz, R., Laufs, U., & Schlüter, K.-D. (2017). Physiological and therapeutic regulation of PCSK9 activity in cardiovascular disease. *Basic Research in Cardiology*, *112*, 32. https://doi.org/10.1007/s00395-017-0619-0

Gwag, T., Meng, Z., Sui, Y., Helsley, R. N., Park, S. H., Wang, S., Greenberg, R. N., & Zhou, C. (2019). Non-nucleoside reverse transcriptase inhibitor efavirenz activates PXR to induce hypercholesterolemia and hepatic steatosis. *Journal of Hepatology*, *70*, 930–940. https://doi.org/10.1016/j.jhep.2018.12.038

Hakkola, J., Rysä, J., & Hukkanen, J. (2016). Regulation of hepatic energy metabolism by the nuclear receptor PXR. *Biochimica et Biophysica Acta (BBA) - Gene Regulatory Mechanisms*, *1859*, 1072–1082. https://doi.org/10.1016/j.bbagrm.2016.03.012

Hassani-Nezhad-Gashti, F., Kummu, O., Karpale, M., Rysä, J., & Hakkola, J. (2019). Nutritional status modifies pregnane X receptor regulated transcriptome. *Scientific Reports*, *9*, 16728. https://doi.org/10.1038/s41598-019-53101-9

Hassani-Nezhad-Gashti, F., Salonurmi, T., Hautajärvi, H., Rysä, J., Hakkola, J., & Hukkanen, J. (2020). Pregnane X receptor activator rifampin increases blood pressure and stimulates plasma renin activity. *Clinical Pharmacology & Therapeutics*, *108*, 856–865. https://doi.org/10.1002/cpt.1871

Hautajärvi, H., Hukkanen, J., Turpeinen, M., Mattila, S., & Tolonen, A. (2018). Quantitative analysis of 4β- and 4α-hydroxycholesterol in human plasma and serum by UHPLC/ESI-HR-MS. *Journal of Chromatography B*, *1100–1101*, 179–186.

He, J., Gao, J., Xu, M., Ren, S., Stefanovic-Racic, M., O'Doherty, R. M., & Xie, W. (2013). PXR ablation alleviates diet-induced and genetic obesity and insulin resistance in mice. *Diabetes*, *62*, 1876–1887. https://doi.org/10.2337/db12-1039

Howe, K., Sanat, F., Thumser, A. E., Coleman, T., & Plant, N. (2011). The statin class of HMG-CoA reductase inhibitors demonstrate differential activation of the nuclear receptors PXR, CAR and FXR, as well as their downstream target genes. *Xenobiotica*, *41*, 519–529. https://doi.org/10.3109/00498254.2011.569773

Hukkanen, J., Rysä, J., Mäkelä, K. A., Herzig, K.-H., Hakkola, J., & Savolainen, M. J. (2015). The effect of pregnane X receptor agonists on postprandial incretin hormone secretion in rats and humans. *Journal of Physiology and Pharmacology*, *66*, 831–839.

Hukkanen, J. (2012). Induction of cytochrome P450 enzymes: A view on human *in vivo* findings. *Expert Review of Clinical Pharmacology*, *5*, 569–585. https://doi.org/10.1586/ecp.12.39

Hukkanen, J., Puurunen, J., Hyötyläinen, T., Savolainen, M. J., Ruokonen, A., Morin-Papunen, L., Orešič, M., Piltonen, T., & Tapanainen, J. S. (2015). The effect of atorvastatin treatment on serum oxysterol concentrations and cytochrome P450 3A4 activity. *British Journal of Clinical Pharmacology*, *80*, 473–479. https://doi.org/10.1111/bcp.12701

Ingelsson, E., Schaefer, E. J., Contois, J. H., McNamara, J. R., Sullivan, L., Keyes, M. J., Pencina, M. J., Schoonmaker, C., Wilson, P. W. F., D'Agostino, R. B., & Vasan, R. S. (2007). Clinical utility of different lipid measures for prediction of coronary heart disease in men and women. *Journal of the American Medical Association*, *298*, 776–785. https://doi.org/10.1001/jama.298.7.776

Inouye, M., Kettunen, J., Soininen, P., Silander, K., Ripatti, S., Kumpula, L. S., Hämäläinen, E., Jousilahti, P., Kangas, A. J., Männistö, S., Savolainen, M. J., Jula, A., Leiviskä, J., Palotie, A., Salomaa, V., Perola, M., Ala-Korpela, M., & Peltonen, L. (2010). Metabonomic, transcriptomic, and genomic variation of a population cohort. *Molecular Systems Biology*, *6*, 441. https://doi.org/10.1038/msb.2010.93

Kallio, M. A., Tuimala, J. T., Hupponen, T., Klemelä, P., Gentile, M., Scheinin, I., Koski, M., Käki, J., & Korpelainen, E. I. (2011). Chipster: User-friendly analysis software for microarray and other high-throughput data. *BMC Genomics*, *12*, 507. https://doi.org/10.1186/1471-2164-12-507

Kasichayanula, S., Boulton, D. W., Luo, W.-L., Rodrigues, A. D., Yang, Z., Goodenough, A., Lee, M., Jemal, M., & LaCreta, F. (2014). Validation of 4β-hydroxycholesterol and evaluation of other endogenous biomarkers for the assessment of CYP3A activity in healthy subjects. *British Journal of Clinical Pharmacology*, *78*, 1122–1134. https://doi.org/10.1111/bcp.12425

Khuseyinova, N., & Koenig, W. (2006). Apolipoprotein A-I and risk for cardiovascular diseases. *Current Atherosclerosis Reports*, *8*, 365–373. https://doi.org/10.1007/s11883-006-0033-9

Kliewer, S. A., Goodwin, B., & Willson, T. M. (2002). The nuclear pregnane X receptor: A key regulator of xenobiotic metabolism. *Endocrine Reviews*, *23*, 687–702. https://doi.org/10.1210/er.2001-0038

Kliewer, S. A., Moore, J. T., Wade, L., Staudinger, J. L., Watson, M. A., Jones, S. A., McKee, D. D., Oliver, B. B., Willson, T. M., Zetterström, R. H., Perlmann, T., & Lehmann, J. M. (1998). An orphan nuclear receptor activated by pregnanes defines a novel steroid signaling pathway. *Cell*, *92*, 73–82. https://doi.org/10.1016/S0092-8674(00)80900-9

Krämer, A., Green, J., Pollard, J., Tugendreich, S., & Tugendreich, S. (2014). Causal analysis approaches in ingenuity pathway analysis. *Bioinformatics (Oxford, England)*, *30*, 523–530. https://doi.org/10.1093/bioinformatics/btt703

Lagace, T. A. (2014). PCSK9 and LDLR degradation: Regulatory mechanisms in circulation and in cells. *Current Opinion in Lipidology*, *25*, 387–393. https://doi.org/10.1097/MOL.0000000000000114

Laufs, U., Dent, R., Kostenuik, P. J., Toth, P. P., Catapano, A. L., & Chapman, M. J. (2019). Why is hypercholesterolaemia so prevalent? A view from evolutionary medicine. *European Heart Journal*, *40*, 2825–2830. https://doi.org/10.1093/eurheartj/ehy479

Li, L., Li, H., Garzel, B., Yang, H., Sueyoshi, T., Li, Q., Shu, Y., Zhang, J., Hu, B., Heyward, S., Moeller, T., Xie, W., Negishi, M., & Wang, H. (2015). SLC13A5 is a novel transcriptional target of the pregnane x receptor and sensitizes drug-induced steatosis in human liver. *Molecular Pharmacology*, *87*, 674–682. https://doi.org/10.1124/mol.114.097287

Li, T., & Chiang, J. Y. L. (2005). Mechanism of rifampicin and pregnane X receptor inhibition of human cholesterol 7 alpha-hydroxylase gene transcription. *American Journal of Physiology. Gastrointestinal and Liver Physiology*, *288*, G74–G84. https://doi.org/10.1152/ajpgi.00258.2004

Lilley, E., Stanford, S. C., Kendall, D. E., Alexander, S. P. H., Cirino, G., Docherty, J. R., George, C. M., Insel, P. A., Izzo, A. A., Ji, Y., Panettieri, R. A., Sobey, C. G., Stefanska, B., Stephens, G., Teixeira, M., & Ahluwalia, A. (2020). ARRIVE 2.0 and the British Journal of pharmacology: Updated guidance for 2020. *British Journal of Pharmacology*, *177*, 3611–3616. https://doi.org/10.1111/bph.15178

Lu, Y., Feskens, E. J. M., Boer, J. M. A., & Müller, M. (2010). The potential influence of genetic variants in genes along bile acid and bile metabolic pathway on blood cholesterol levels in the population. *Atherosclerosis*, *210*, 14–27. https://doi.org/10.1016/j.atherosclerosis.2009.10.035

Luoma, P. V., Reunanen, M. I., & Sotaniemi, E. A. (1979). Changes in serum triglyceride and cholesterol levels during long-term phenytoin treatment for epilepsy. *Acta Medica Scandinavica*, *206*, 229–231. https://doi.org/10.1111/j.0954-6820.1979.tb13500.x

Lütjohann, D., Hahn, C., Prange, W., Sudhop, T., Axelson, M., Sauerbruch, T., Bergmann, K., & Reichel, C. (2004). Influence of rifampin on serum markers of cholesterol and bile acid synthesis in men.

International Journal of Clinical Pharmacology and Therapeutics, *42*, 307–313. https://doi.org/10.5414/CPP42307

Mantel-Teeuwisse, A. K., Kloosterman, J. M. E., Maitland-van der Zee, A. H., Klungel, O. H., Porsius, A. J., & de Boer, A. (2001). Drug-induced lipid changes. *Drug Safety*, *24*, 443–456. https://doi.org/10.2165/00002018-200124060-00003

Marmugi, A., Lasserre, F., Beuzelin, D., Ducheix, S., Huc, L., Polizzi, A., Chetivaux, M., Pineau, T., Martin, P., Guillou, H., & Mselli-Lakhal, L. (2014). Adverse effects of long-term exposure to bisphenol A during adulthood leading to hyperglycaemia and hypercholesterolemia in mice. *Toxicology*, *325*, 133–143. https://doi.org/10.1016/j.tox.2014.08.006

Marschall, H.-U., Wagner, M., Zollner, G., Fickert, P., Diczfalusy, U., Gumhold, J., Silbert, D., Fuchsbichler, A., Benthin, L., Grundström, R., Gustafsson, U., Sahlin, S., Einarsson, C., & Trauner, M. (2005). Complementary stimulation of hepatobiliary transport and detoxification systems by rifampicin and ursodeoxycholic acid in humans. *Gastroenterology*, *129*, 476–485. https://doi.org/10.1016/j.gastro.2005.05.009

Meng, Z., Gwag, T., Sui, Y., Park, S.-H., Zhou, X., & Zhou, C. (2019). The atypical antipsychotic quetiapine induces hyperlipidemia by activating intestinal PXR signaling. *JCI Insight*, *4*, e125657. https://doi.org/10.1172/jci.insight.125657

Meyer, J. M., & Koro, C. E. (2004). The effects of antipsychotic therapy on serum lipids: A comprehensive review. *Schizophrenia Research*, *70*, 1–17. https://doi.org/10.1016/j.schres.2004.01.014

Miettinen, T. A., Tilvis, R. S., & Kesäniemi, Y. A. (1989). Serum cholestanol and plant sterol levels in relation to cholesterol metabolism in middle-aged men. *Metabolism*, *38*, 136–140. https://doi.org/10.1016/0026-0495(89)90252-7

Müjgan Aynaci, F., Orhan, F., Orem, A., Yildirmis, S., & Gedik, Y. (2001). Effect of antiepileptic drugs on plasma lipoprotein (a) and other lipid levels in childhood. *Journal of Child Neurology*, *16*, 367–369. https://doi.org/10.1177/088307380101600511

Nagaoka, S., Miyazaki, H., Aoyama, Y., & Yoshida, A. (1990). Effects of dietary polychlorinated biphenyls on cholesterol catabolism in rats. *The British Journal of Nutrition*, *64*, 161–169. https://doi.org/10.1079/BJN19900018

Nicholson, A., Reifsnyder, P. C., Malcolm, R. D., Lucas, C. A., MacGregor, G. R., Zhang, W., & Leiter, E. H. (2010). Diet-induced obesity in two C57BL/6 substrains with intact or mutant nicotinamide nucleotide transhydrogenase (Nnt) gene. *Obesity*, *18*, 1902–1905. https://doi.org/10.1038/oby.2009.477

Ohnhaus, E. E., Kirchhof, B., & Peheim, E. (1979). Effect of enzyme induction on plasma lipids using antipyrine, phenobarbital, and rifampicin. *Clinical Pharmacology and Therapeutics*, *25*, 591–597. https://doi.org/10.1002/cpt1979255part1591

Percie du Sert, N., Hurst, V., Ahluwalia, A., Alam, S., Avey, M. T., Baker, M., Browne, W. J., Clark, A., Cuthill, I. C., Dirnagl, U., Emerson, M., Garner, P., Holgate, S. T., Howells, D. W., Karp, N. A., Lazic, S. E., Lidster, K., MacCallum, C. J., Macleod, M., & Würbel, H. (2020). The ARRIVE guidelines 2.0: Updated guidelines for reporting animal research. *PLoS Biology*, *18*(7), e3000410. https://doi.org/10.1371/journal.pbio.3000410

Ricketts, M.-L., Boekschoten, M. V., Kreeft, A. J., Hooiveld, G. J. E. J., Moen, C. J. A., Müller, M., Frants, R. R., Kasanmoentalib, S., Post, S. M., Princen, H. M. G., Porter, J. G., Katan, M. B., Hofker, M. H., & Moore, D. D. (2007). The cholesterol-raising factor from coffee beans, cafestol, as an agonist ligand for the farnesoid and pregnane X receptors. *Molecular Endocrinology (Baltimore, Md.)*, *21*, 1603–1616. https://doi.org/10.1210/me.2007-0133

Roth, A., Looser, R., Kaufmann, M., Blättler, S. M., Rencurel, F., Huang, W., Moore, D. D., & Meyer, U. A. (2008). Regulatory cross-talk between drug metabolism and lipid homeostasis: Constitutive androstane receptor and pregnane X receptor increase Insig-1 expression.

Molecular Pharmacology, *73*, 1282–1289. https://doi.org/10.1124/mol.107.041012

Roth, G. A., Forouzanfar, M. H., Moran, A. E., Barber, R., Nguyen, G., Feigin, V. L., Naghavi, M., Mensah, G. A., & Murray, C. J. L. (2015). Demographic and epidemiologic drivers of global cardiovascular mortality. *The New England Journal of Medicine*, *372*, 1333–1341. https://doi.org/10.1056/NEJMoa1406656

Rysä, J., Buler, M., Savolainen, M. J., Ruskoaho, H., Hakkola, J., & Hukkanen, J. (2013). Pregnane X receptor agonists impair postprandial glucose tolerance. *Clinical Pharmacology & Therapeutics*, *93*, 556–563. https://doi.org/10.1038/clpt.2013.48

Sahebkar, A., Simental-Mendía, L. E., Guerrero-Romero, F., Golledge, J., & Watts, G. F. (2015). Effect of statin therapy on plasma proprotein convertase subtilisin kexin 9 (PCSK9) concentrations: A systematic review and meta-analysis of clinical trials. *Diabetes, Obesity and Metabolism*, *17*, 1042–1055. https://doi.org/10.1111/dom.12536

Schlitt, A., Blankenberg, S., Yan, D., Von Gizycki, H., Buerke, M., Werdan, K., Bickel, C., Lackner, K. J., Meyer, J., Rupprecht, H. J., & Jiang, X. C. (2006). Further evaluation of plasma sphingomyelin levels as a risk factor for coronary artery disease. *Nutrition and Metabolism*, *3*, 1–8.

Seidah, N. G., Awan, Z., Chrétien, M., & Mbikay, M. (2014). PCSK9: A key modulator of cardiovascular health. *Circulation Research*, *114*, 1022–1036. https://doi.org/10.1161/CIRCRESAHA.114.301621

Sever, N., Yang, T., Brown, M. S., Goldstein, J. L., & DeBose-Boyd, R. A. (2003). Accelerated degradation of HMG CoA reductase mediated by binding of insig-1 to its sterol-sensing domain. *Molecular Cell*, *11*, 25–33. https://doi.org/10.1016/S1097-2765(02)00822-5

Shimano, H., & Sato, R. (2017). SREBP-regulated lipid metabolism: Convergent physiology - divergent pathophysiology. *Nature Reviews. Endocrinology*, *13*, 710–730. https://doi.org/10.1038/nrendo.2017.91

Soininen, P., Kangas, A. J., Würtz, P., Suna, T., & Ala-Korpela, M. (2015). Quantitative serum nuclear magnetic resonance metabolomics in cardiovascular epidemiology and genetics. *Circulation. Cardiovascular Genetics*, *8*, 192–206. https://doi.org/10.1161/CIRCGENETICS.114.000216

Soininen, P., Kangas, A. J., Würtz, P., Tukiainen, T., Tynkkynen, T., Laatikainen, R., Järvelin, M. R., Kähönen, M., Lehtimäki, T., Viikari, J., Raitakari, O. T., Savolainen, M. J., & Ala-Korpela, M. (2009). High-throughput serum NMR metabonomics for cost-effective holistic studies on systemic metabolism. *The Analyst*, *134*, 1781–1785. https://doi.org/10.1039/b910205a

Spann, N. J., Garmire, L. X., McDonald, J. G., Myers, D. S., Milne, S. B., Shibata, N., Reichart, D., Fox, J. N., Shaked, I., Heudobler, D., Raetz, C. R. H., Wang, E. W., Kelly, S. L., Sullards, M. C., Murphy, R. C., Merrill, A. H. Jr., Brown, H. A., Dennis, E. A., Li, A. C., & Glass, C. K. (2012). Regulated accumulation of desmosterol integrates macrophage lipid metabolism and inflammatory responses. *Cell*, *151*, 138–152. https://doi.org/10.1016/j.cell.2012.06.054

Spruiell, K., Richardson, R. M., Cullen, J. M., Awumey, E. M., Gonzalez, F. J., & Gyamfi, M. A. (2014). Role of Pregnane X receptor in obesity and glucose homeostasis in male mice. *Journal of Biological Chemistry*, *289*, 3244–3261. https://doi.org/10.1074/jbc.M113.494575

Temel, R. E., & Brown, J. M. (2015). A new model of reverse cholesterol transport: enTICEing strategies to stimulate intestinal cholesterol excretion. *Trends in Pharmacological Sciences*, *36*, 440–451. https://doi.org/10.1016/j.tips.2015.04.002

Toye, A. A., Lippiat, J. D., Proks, P., Shimomura, K., Bentley, L., Hugill, A., Mijat, V., Goldsworthy, M., Moir, L., Haynes, A., Quarterman, J., Freeman, H. C., Ashcroft, F. M., & Cox, R. D. (2005). A genetic and physiological study of impaired glucose homeostasis control in C57BL/6J mice. *Diabetologia*, *48*, 675–686. https://doi.org/10.1007/s00125-005-1680-z

van der Wulp, M. Y. M., Verkade, H. J., & Groen, A. K. (2013). Regulation of cholesterol homeostasis. *Molecular and Cellular Endocrinology*, *368*, 1–16. https://doi.org/10.1016/j.mce.2012.06.007

Wang, Q., Jokelainen, J., Auvinen, J., Puukka, K., Keinänen-Kiukaanniemi, S., Järvelin, M.-R., Kettunen, J., Mäkinen, V. P., & Ala-Korpela, M. (2019). Insulin resistance and systemic metabolic changes in oral glucose tolerance test in 5340 individuals: An interventional study. *BMC Medicine*, *17*, 217. https://doi.org/10.1186/s12916-019-1440-4

Warden, B. A., Fazio, S., & Shapiro, M. D. (2019). The PCSK9 revolution: Current status, controversies, and future directions. *Trends in Cardiovascular Medicine*, *30*, 179–185.

Weusten-Van der Wouw, M. P. M. E., Katan, M. B., Viani, R., Huggett, A. C., Liardon, R., Lund-Larsen, P. G., Thelle, D. S., Ahola, I., & Aro, A. (1994). Identity of the cholesterol-raising factor from boiled coffee and its effects on liver function enzymes. *Journal of Lipid Research*, *35*, 721–733. https://doi.org/10.1016/S0022-2275(20)41169-1

Würtz, P., Kangas, A. J., Soininen, P., Lawlor, D. A., Davey Smith, G., & Ala-Korpela, M. (2017). Quantitative serum nuclear magnetic resonance metabolomics in large-scale epidemiology: A primer on-omic technologies. *American Journal of Epidemiology*, *186*, 1084–1096. https://doi.org/10.1093/aje/kwx016

Würtz, P., & Soininen, P. (2020). Reply to: "Methodological issues regarding: 'A third of nonfasting plasma cholesterol is in remnant lipoproteins: Lipoprotein subclass profiling in 9293 individuals'". *Atherosclerosis*, *302*, 59–61. https://doi.org/10.1016/j.atherosclerosis.2020.03.028

Würtz, P., Wang, Q., Soininen, P., Kangas, A. J., Fatemifar, G., Tynkkynen, T., Tiainen, M., Perola, M., Tillin, T., Hughes, A. D., Mäntyselkä, P., Kähönen, M., Lehtimäki, T., Sattar, N., Hingorani, A. D., Casas, J. P., Salomaa, V., Kivimäki, M., Järvelin, M. R., & Ala-Korpela, M. (2016). Metabolomic profiling of statin use and genetic inhibition of HMG-CoA reductase. *Journal of the American College of Cardiology*, *67*, 1200–1210. https://doi.org/10.1016/j.jacc.2015.12.060

Xie, W., Barwick, J. L., Downes, M., Blumberg, B., Simon, C. M., Nelson, M. C., Neuschwander-Tetri, B. A., Brunt, E. M., Guzelian, P. S., & Evans, R. M. (2000). Humanized xenobiotic response in mice expressing nuclear receptor SXR. *Nature*, *406*, 435–439. https://doi.org/10.1038/35019116

Yang, C., McDonald, J. G., Patel, A., Zhang, Y., Umetani, M., Xu, F., Westover, E. J., Covey, D. F., Mangelsdorf, D. J., Cohen, J. C., & Hobbs, H. H. (2006). Sterol intermediates from cholesterol biosynthetic pathway as liver X receptor ligands. *Journal of Biological Chemistry*, *281*, 27816–27826. https://doi.org/10.1074/jbc.M603781200

Yoshii, Y., Furukawa, T., Saga, T., & Fujibayashi, Y. (2015). Acetate/acetyl-CoA metabolism associated with cancer fatty acid synthesis: Overview and application. *Cancer Letters*, *356*, 211–216. https://doi.org/10.1016/j.canlet.2014.02.019

Zhou, C. (2016). Novel functions of PXR in cardiometabolic disease. *Biochimica et Biophysica Acta, Gene Regulatory Mechanisms*, *1859*, 1112–1120. https://doi.org/10.1016/j.bbagrm.2016.02.015

Zhou, C., King, N., Chen, K. Y., & Breslow, J. L. (2009). Activation of PXR induces hypercholesterolemia in wild-type and accelerates atherosclerosis in apoE deficient mice. *Journal of Lipid Research*, *50*, 2004–2013. https://doi.org/10.1194/jlr.M800608-JLR200

Zhou, J., Zhai, Y., Mu, Y., Gong, H., Uppal, H., Toma, D., Ren, S., Evans, R. M., & Xie, W. (2006). A novel pregnane X receptor-mediated and sterol regulatory element-binding protein-independent lipogenic pathway. *The Journal of Biological Chemistry*, *281*, 15013–15020. https://doi.org/10.1074/jbc.M511116200

SUPPORTING INFORMATION

Additional supporting information may be found online in the Supporting Information section at the end of this article.